Theoretical and Experimental Vibrational Modes of the Borane Pyridine Complex

By

Benjamin Wade Stratton

A thesis submitted to the faculty of The University of Mississippi in partial fulfillment of the requirements of the Sally McDonnell Barksdale Honors College

Oxford

May 2019

Approved By:

_____

Advisor: Professor Nathan Hammer

_____

Reader: Professor Jason Ritchie

_____

Reader: Professor Jared Delcamp

Acknowledgements

I would like to thank several people who made this project possible by supporting me and mentoring me through this process. I would first like to thank Dr. Hammer for allowing me to work in his lab and starting me on my path in physical chemistry. His advice and instructions lead me through this paper every step of the way. Secondly, I would like to thank Shane Autry, Ashley Williams, Leigh Anna Hunt, Austin Dorris, and April Steen all of whom helped me through this thesis in some way. The graduate students helped me take data, run calculations, and reassured me that I would be able to complete this project. Without their help I would not have been able to complete it. Lastly, I would like to thank my parents Terry and Alicia Stratton for supporting me throughout my life and continuing to cheer me on as I take my academic career to the next step.

Abstract

Benjamin Wade Stratton: Theoretical and Experimental Vibrational Modes of the Borane Pyridine Complex

(Under the direction of Dr. Nathan Hammer)

The Borane Pyridine complex is a molecule that contains a dative bond between the boron and nitrogen atoms. A dative bond is a type of covalent bonding that occurs when both electrons come from the same atom. The B-N bond has been studied in several other molecules such as ammonia borane and determining the frequency at which this bond vibrates has been a topic of interest studied in these molecules as well as several others. This complex has another factor that makes it of interest, which is the pyridine ring it contains. While several studies on B-N bonds and pyridine have been performed separately in the Hammer lab this molecule contains both which makes it especially interesting. Borane pyridine, along with pyridine, was studied here using Raman spectroscopy and theoretical density functional theory calculations to characterize the vibrational modes. B3LYP and M06-2X methods were used along with 6-311+G(*d*,*p*), aug-cc-pVDZ, and aug-cc-pVTZ basis sets. It was found both theoretically and experimentally that pyridines interaction with the borane group causes its vibrational modes to be blue shifted. It was also found that when pyridine interacts with water through hydrogen bonding that its modes are also blue shifted, but this shift is smaller.

Table of Contents

Chapter 1: Chemical Bonds

1.1 Bonding and Chemical Interactions

Chemical bonds occur when there is a sharing of electrons between atoms. Atoms are made up of positive and negative particles called protons and electrons and neutral particles called neutrons. The electron is the main particle that participates in bonding as they can generally be shared or transferred by atoms or molecules.[1] The two main kinds of bonding are covalent bonds, which occur when electrons are shared, and ionic bonds, which occur when electrons are transferred. Covalent bonds generally occur between nonmetals such as oxygen, carbon, or nitrogen and involve two atoms sharing a pair of electrons. This type of bonding lowers the potential energy of both atoms involved which is why it occurs. Covalent bonding can be further split into polar and nonpolar covalent bonding depending on the difference in electronegativity of the atoms participating in the bonding. If the atoms have very similar electronegativities, such as a bond between carbon and carbon or carbon and hydrogen, the bond is said to be a nonpolar covalent bond.[2] If the difference in the atoms electronegativities is large, then the bond is said to be a nonpolar covalent bond, which can result in regions of partial positive and negative charges. Bonds can also occur when electrons are transferred between atoms in ionic bonding. Ionic bonds generally occur between a metal that donates electrons and a nonmetal that accepts those electrons. These metals can be seen on the left side of the periodic table and in their natural state have either one or two electrons occupying their valence shell. By having only 1 or 2

electrons in the valence orbital these atoms are unstable as they do not have a full octet. On the other side of the periodic table are the nonmetals, such as oxygen or chlorine, that have 6 or 7 valence electrons and are also unstable due to the fact that they do not have a completed octet. The metals with too many electrons can donate their electrons to the nonmetals which results in both atoms having a completed octet and forming an ionic bond that bring both atoms into lower energy states.[1]

1.2 Dative Bonding

The type of bonding exhibited in the borane pyridine complex between the boron and nitrogen atoms is a type of covalent bonding called coordinate or dative bonding. In this type of covalent bond both electrons come from the same atom, which in this molecule both electrons come from the nitrogen atom and are shared with the boron atom. This bond is a polar covalent bond as the nitrogen atom has an electronegativity of 3.04 while boron has an electronegativity of 2.04.[3] Many atoms form bonds according to the octet rule, which is a rule that states that most atoms form bonds in order to have 8 electrons in their valence orbital. This is seen best in ionic bonding where an atom that has 1 valence electron, like sodium, can lose its electron to an atom that has 7 valence electrons, like chlorine. When sodium's electron transfers to chlorine both atoms now have 8 electrons in their valence shell resulting in a more stable or less energetic state, which is favorable. Boron is an atom that does not obey the octet rule as it only has 3 electrons in its valence shell which causes it to only be able to form 3 bonds and have 6 electrons in its valence orbital. Because of this boron often forms dative bonds where it is acting as the receptor of an electron pair, or a Lewis acid. Some other molecule must donate these electrons because boron does not

have any electrons to form a normal covalent bond with. The atom or molecule that donates the electrons is considered to be a Lewis base, so molecules with dative bonds in them are also Lewis acid base pairs. Nitrogen and phosphorus are two common atoms that will form dative bonds with boron in complexes such as ammonia borane (maybe insert pic of ammonia borane). The molecule of interest is borane pyridine, which contains a boron nitrogen (B-N) dative bond. The nitrogen from the pyridine molecule, acting as the Lewis base, donates electrons to borane and forms the borane pyridine complex. Dative bonds, especially B-N dative bond, are commonly used in synthesis as they can be used as building blocks for larger more complicated molecules.

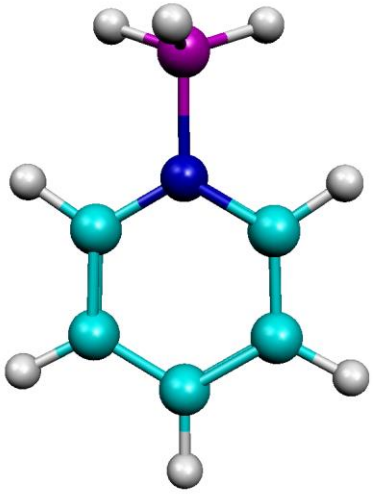

Figure 1.1- A picture showing the borane pyridine molecule. The purple atom represents boron while the blue atoms represents nitrogen, which shows the B-N bond.

The borane pyridine molecule, shown in figure 1.1 above, is interesting to study because of its B-N bond since the frequency of this bond has been studied for many years with many different molecules. The frequency has been assigned in molecules like ammonia borane at 799 cm^{-1}, or in molecules like N-

methyliminodiacetic acid (MIDA) at 560-650 cm^{-1}.[5,6] There have been large discrepancies in the position of the B-N bond in different molecules with some values being as low as 600 cm^{-1} and some molecules having modes as high as 1200-1. Borane pyridine has a B-N bond that can be characterized and compared to other molecules, but it also has a pyridine molecule. Here the vibrational modes of borane pyridine are compared to the vibrational modes of pyridine in order to see the effect of the borane group on pyridine's vibrational modes. The effects of hydrogen bonding are also compared to these results.

Chapter 2: Spectroscopy and Experimental Instrumentation

2.1 Spectroscopy

Spectroscopy is defined as the study of light-matter interactions and is used in many studies and is used in everything from physics, biology, and especially chemistry. Light is a form of electromagnetic radiation that exists on a spectrum and depending on what wavelength and energy light is interacting with matter, different types of transitions can occur and different information about the atoms or molecules can be gathered. Light acts as both a wavelength and a particle so it cannot be described as just one or the other. It can be described as both a wave of oscillating magnetic and electric fields and a distinct packet of quanta or a photon. The energy of a photon of light is inversely proportional to its wavelength meaning that the shorter a wavelength of light is the higher energy it will have. This is shown by the equation below, which is also known as the Planck-Einstein relation.

$$E = h\upsilon = \frac{hc}{\lambda}$$

This equation relates the energy of a photon to its wavelength as the other two values in the equation are constants and do not change. Planck's constant, h with a value of $6.626*10^{-34}$ J*s, and the speed of light, c with a value of $3.0*10^{8}$ m/s, do not change, so the only thing that can change the energy of a photon is its wavelength. The relation also makes the

dual nature of light apparent by showing how the energy of light can be described through frequency or through wavelength. The electromagnetic spectrum has a large range of different light that interacts with matter differently. The spectrum can be seen in Figure 2.1.1 below with the highest energy lowest wavelength light being at the left and the highest wavelength lowest energy light being at the right of the spectrum.

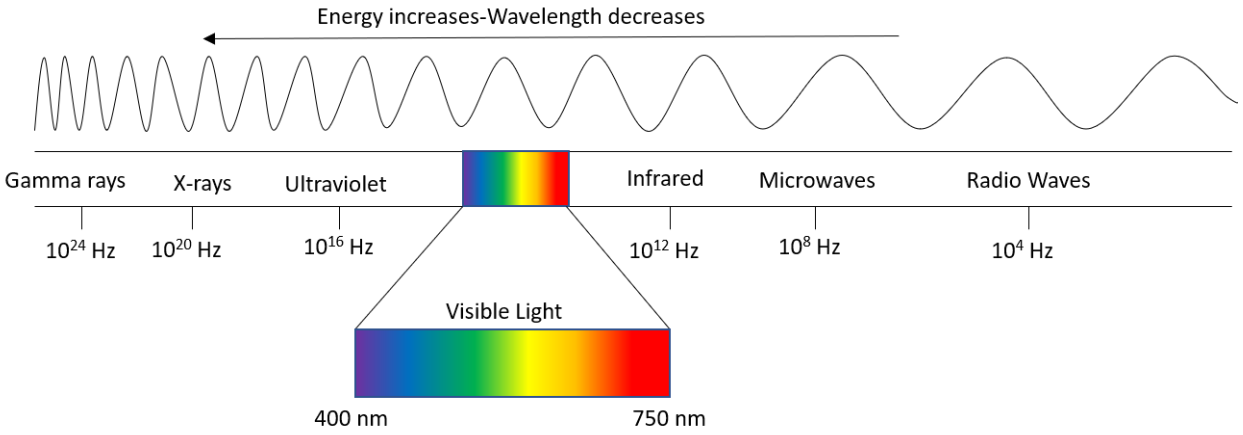

Figure 2.1.: Electromagnetic Spectrum- A figure showing the electromagnetic spectrum in measurements of frequency and wavelength. Visible light only occupies a small portion of the spectrum from around 400-700 nm.[8]

The different wavelengths of light are all useful for different kinds of spectroscopy. Lesser used wavelengths include gamma and x-rays since these wavelengths are vey high in energy. Gamma rays can be used to rearrange nuclear particles and X-rays can be used to eject core electrons from an atom or molecule, but since these wavelengths are so high in energy their use is limited. More popular spectroscopies are those from the ultraviolet and visible, UV-Vis, regions and IR spectroscopy. UV-Vis spectroscopy works by exciting molecules into higher electronic states. This spectroscopy is often used with the Beer-Lambert law, $A = \varepsilon bc$, in order to determine the concentration of a substance by measuring its absorbance.[7] In the Beer-Lambert law A represents absorbance, ε is the molar

absorptivity constant, b is the path length, and finally c is the concentration. IR spectroscopy is a vibrational spectroscopy that uses infrared light to identify the vibrational frequencies of certain functional groups, which allows the structure of the molecule to be known. Both UV-Vis spectroscopy and IR spectroscopy are types of absorptions spectroscopy, but UV-Vis spectroscopy is more useful for quantitative analysis while IR spectroscopy is more useful for qualitative spectroscopy. Another important difference to note is that IR and other vibrational spectroscopies can only be applied to molecules as only molecules have vibrational energy levels. Atoms do not have vibrational energy levels and therefore cannot be studied using any vibrational spectroscopy, but UV-Vis can be used to study atoms as atoms do still have electronic energy levels. Microwaves are another type of spectroscopy that can only work on molecules as it studies the rotational energy levels that atoms do not have.

2.1.1 Vibrational Spectroscopy

There are four energy levels that can be excited and undergo an energy transition. These four energy levels are Translational, Rotational, Vibrational, and Electronic in order of increasing energy and size of transition. As previously discussed, the various wavelengths of light from the electromagnetic spectrum can be matched to the kind of transition that they induce. UV-Vis light causes electronic transitions while IR light causes vibrational transitions and microwaves cause rotational transitions. Raman spectroscopy, which will be discussed later, is another type of vibrational spectroscopy. Vibrational energy levels and transitions are based on the harmonic oscillator model, which models the

molecule as if it was on a spring or oscillator. In classical physics the force acting on a spring can be described by Hooke's law,

$$F = -kx$$

Where k is the force constant and x is the measurement of displacement. The force of the spring can also be set equal to the potential energy by another equation, assuming that $F = -\frac{dV}{dx}$,

$$V = 1/2\ kx^2$$

V is the harmonic potential and the equation represents an energy well in the shape of a parabola. The harmonic oscillator model creates a harmonic energy well that represents the electronic energy level of the molecule, and in these energy wells there are vibrational energy levels that appear inside the energy well. These energy levels can be represented by the equation

$$E_v = \left(v + \frac{1}{2}\right) hv_0$$

Where v is the frequency h is Planck's constant and v is the vibrational quantum number (v=0,1,2,…∞). This equation shows where the vibrational energy levels will be on the harmonic energy well and shows the distance between the vibrational energy levels as in the harmonic oscillator model the vibrational states are evenly spaced from each other forever. The vibrational quantum number can be calculated so that the vibrational energy level the molecule is in can be known. It can be calculated according to this equation

$$v_0 = \frac{1}{2\pi}\sqrt{\frac{k}{\mu}}$$

Where k is the spring constant described earlier and μ is the reduced mass of the molecule. An example of a harmonic energy well is shown below with the vibrational energy levels being represented as n. The figure also shows how the transition energy does not change as the vibrational state increases.

The harmonic oscillator is a model which means that it makes some assumptions to accurately show how something works. In real life the molecular oscillator is not harmonic but anharmonic because the vibrational amplitudes can become large and the harmonic oscillator is no longer a good model. In the anharmonic oscillator the vibrational energy levels get closer to each other as they get higher, and the well is no longer a parabola but looks like a parabola on one side while flattening out on the other side. An example of an anharmonic energy well can be seen below.

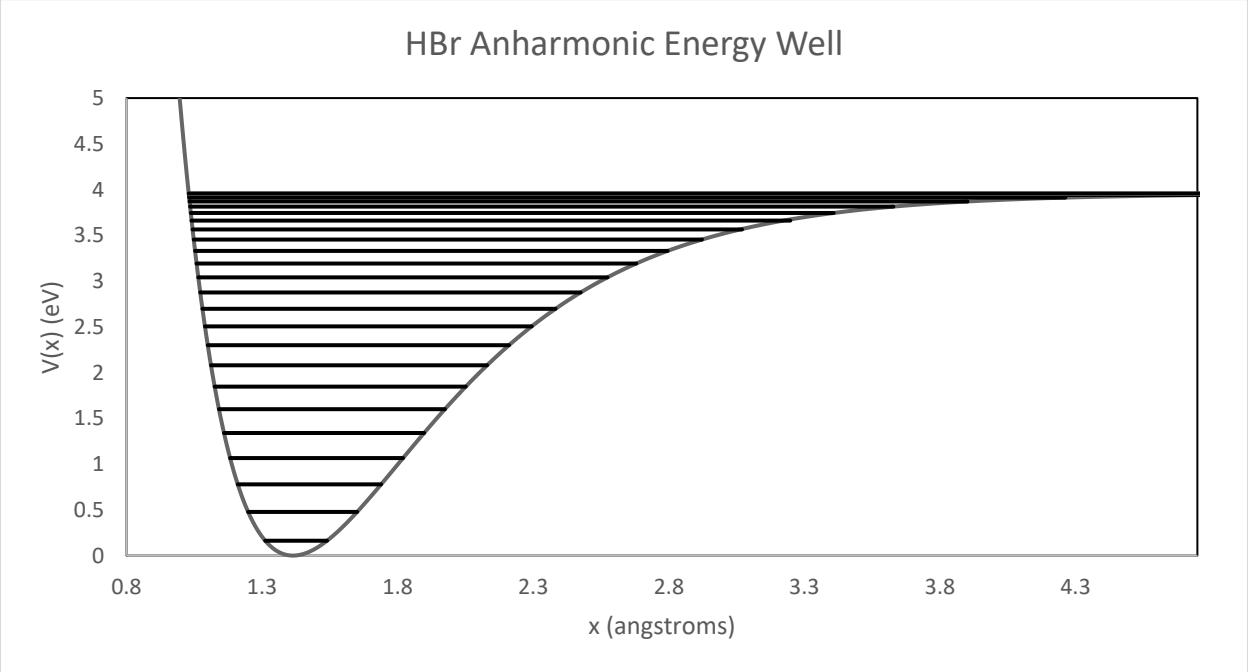

Figure 2.3- An anharmonic energy well.

This anharmonic energy well is made from the HBr molecule and has obvious differences from the harmonic energy well. The vibrational energy levels get closer together as the vibrational state increase and the shape is no longer a parabola, which makes this model more accurate.

2.2 Raman Spectroscopy

Raman scattering was discovered in 1928 by Sir Chandrashekhara Venkata Raman, and it is the main theoretical principle behind Raman spectroscopy. Several different things can happen when light hits matter, and two popular possibilities are that the light is absorbed as in IR spectroscopy, it is scattered as in Raman spectroscopy. IR and Raman spectroscopy are both types of vibrational spectroscopy as they both interact with a molecule's vibrational energy levels. Where IR spectroscopy requires a change in dipole moment for a molecule to be IR active Raman spectroscopy requires a molecule to have a change in polarizability for a molecule to be Raman active. This change in polarizability often comes from a change in a molecules bond length when it vibrates. The change in bond length leads to a distortion of the electron cloud, and therefore electron density, which changes the molecules polarizability. In a molecule like CO_2 which has symmetric and asymmetric vibrational stretching modes the symmetric stretch will be Raman active, but the asymmetric stretch will be IR active. In the symmetric stretch the bond length of the molecule changes and produces a change in polarizability, but the dipole moment does not

change as both oxygen atoms move the same distance away from the carbon atom. However, in the asymmetric stretch the one oxygen atom gets closer to the carbon than the other oxygen atom, which creates a change in dipole moment making the stretch IR active, but since the distance between the two oxygens does not change there is no change in polarizability making the stretch Raman inactive. Many vibrational modes are either IR or Raman active which makes the two spectroscopies useful to use in compliment to each other so that a full view of a molecules vibrational modes can be obtained.

Raman spectroscopy involves the scattering of light which can happen several different ways. The scattering can either be elastic, meaning that the photon was absorbed and emitted without any difference in the molecule's final energy level, or inelastic, which means that the molecules energy level will be changed in some way due to the effect of the photon. The two types of elastic scattering are Mie scattering and Rayleigh scattering. Mie scattering occurs when the particle scattering the light is as big or bigger than the wavelength of the incident light.[10] This is not a common occurrence and does not play a role at all in Raman spectroscopy as most chemicals studied are much smaller than the incident wavelength. Rayleigh scattering occurs when the particle scattering the light is smaller than the wavelength of the light that hits the particle. Rayleigh scattering is an elastic process which means that the incident light and the scattered light will be the same wavelength. While Rayleigh scattering is the most common form of scattering the type of scattering that allows Raman spectroscopy to occur is inelastic scattering. It is estimated that every one in a million photons interacts inelastically with molecules when a light is shone on them. The two types of scattering that make up Raman scattering are Stokes and Anti-Stokes scattering. In stokes scattering the photon hits the molecule and loses some

energy while the molecule gains some of that energy. In contrast in Anti-Stokes scattering the photon interacts with the molecule and the molecule loses energy while the photon gains energy. A diagrams of the three ways light can be scattered is shown below

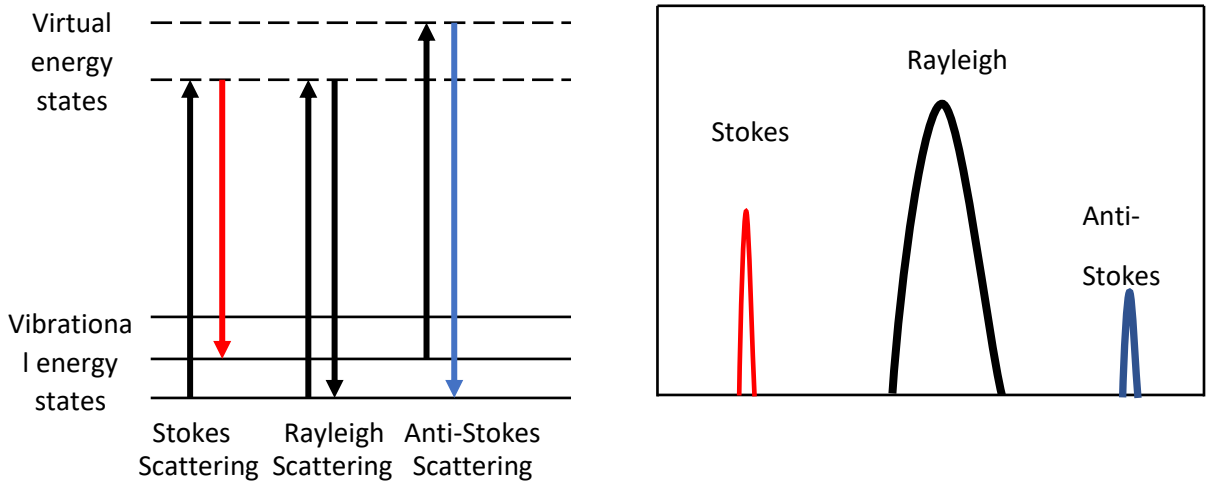

Figure 2.4- A diagram showing elastic Rayleigh scattering versus inelastic Raman scattering (Stokes and Anti-Stokes).[11]

For Rayleigh scattering this figure shows the molecule being excited into a virtual energy state when the photon interacts with it, and then it shows the molecule coming back down to the same energy level when the light is scattered. This figure is especially helpful because it also shows the relative frequency that all of the types of scattering occur. Rayleigh scattering occurs the most and this is obvious because it is the largest peak on the chart. Figure 2.4 also shows the stokes shift going to a virtual state when excited by a photon, but the molecule absorbs some of the photons energy so when the molecule comes back down it occupies a higher energy state than it was originally in. The loss of the photons energy to the molecule is also shown by the returning arrow being red, which is a higher wavelength that has less energy than the other colors in the visible spectrum. The starting arrow is black so it would be better if the starting arrow had been green and changed to red

signaling a loss of energy, but traditionally a shift to lower energy is referred to as a red shift while a shift to higher energy is referred to as a blue shift. These terms are used to describe frequency changes in vibrational modes when comparing two spectra that may have similar vibrational modes. The Anti-Stokes shift is blue because of the blue shift reference as the molecule losses some energy to the photon and the light that is scattered will have a lower wavelength than the incident light. Anti-Stokes scattering is the least common kind of scattering, which is shown in the figure as it has the smallest peak, because it requires that the molecule that the photon is interacting with exist in an excited state. This is rare because at room temperature most molecules exist at the ground state, so in order for Anti-Stokes scattering to occur an inelastic interaction must occur, which is estimated to be one in a million, with a molecule that does not exist in the ground state. This combination of unlikely factors results in Anti-Stokes scattering being very rare, but the occurrence of Anti-Stokes scattering can be increased if the temperature of the system is increased.

2.2.1 Vibrational Modes

Molecules that are Raman or IR active exhibit vibrational modes that correspond to a specific stretch or bend that can be identified by its frequency. These modes can have several different kinds of vibrational motions depending or whether the mode is a stretching or bending mode. Stretching modes change the length of the bonds while keeping the bond angles the same while bending modes change the bond angle while keeping the bond length the same. There are two stretching modes, symmetric and asymmetric stretching, and several different types of bending modes, which include rocking, scissoring, wagging, and twisting. These modes are shown in the figure below.

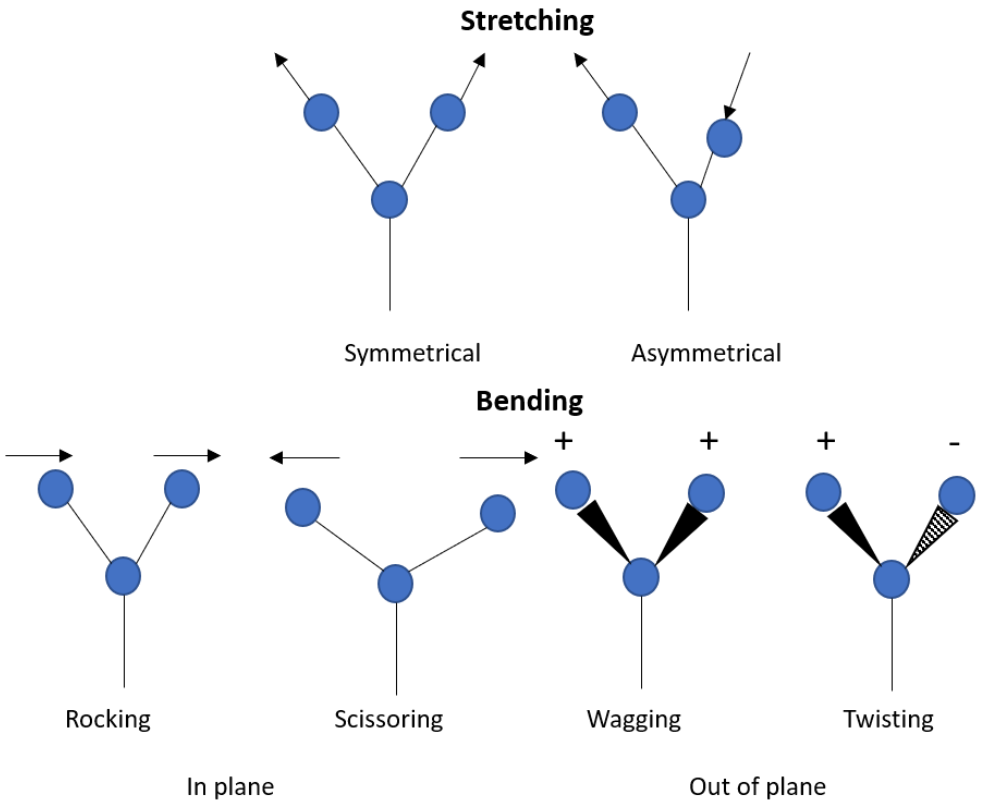

Figure 2.5- A figure showing the how the different vibrational modes mentioned earlier actually move.[12]

Bending modes tend to be much lower in frequency than stretching modes and in IR spectroscopy they are often used in what is referred to as the fingerprint region, which can be helpful in differentiating organic materials or even amino acids in different conformations.[13] Bending modes are rarely seen in Raman spectroscopy because they do not change the bond length, so the polarizability does not change. For this same reason there are also not many asymmetric stretches seen in Raman spectroscopy because while the bond length does change it changes in the same manner for both molecules, meaning that the total distance does not change. In symmetric stretching modes both bond lengths change in the same direction which will change the polarizability of the molecule, so most of the vibrational modes seen in Raman spectroscopy are symmetric stretching modes. The

frequencies at which most common modes occur in IR or Raman spectroscopy can be found online or in scientific journals, but for a molecule that has not had much research on its vibrational modes or if the molecule has some rare bond these modes might not be known. For example, the B-N stretch studied in this paper has been studied in several molecules and has been characterized in those molecules, but the borane pyridine molecule has not had its vibrational modes characterized and the B-N stretch from this molecule can be compared to the stretches in other molecules.

2.3 Raman Instrumentation

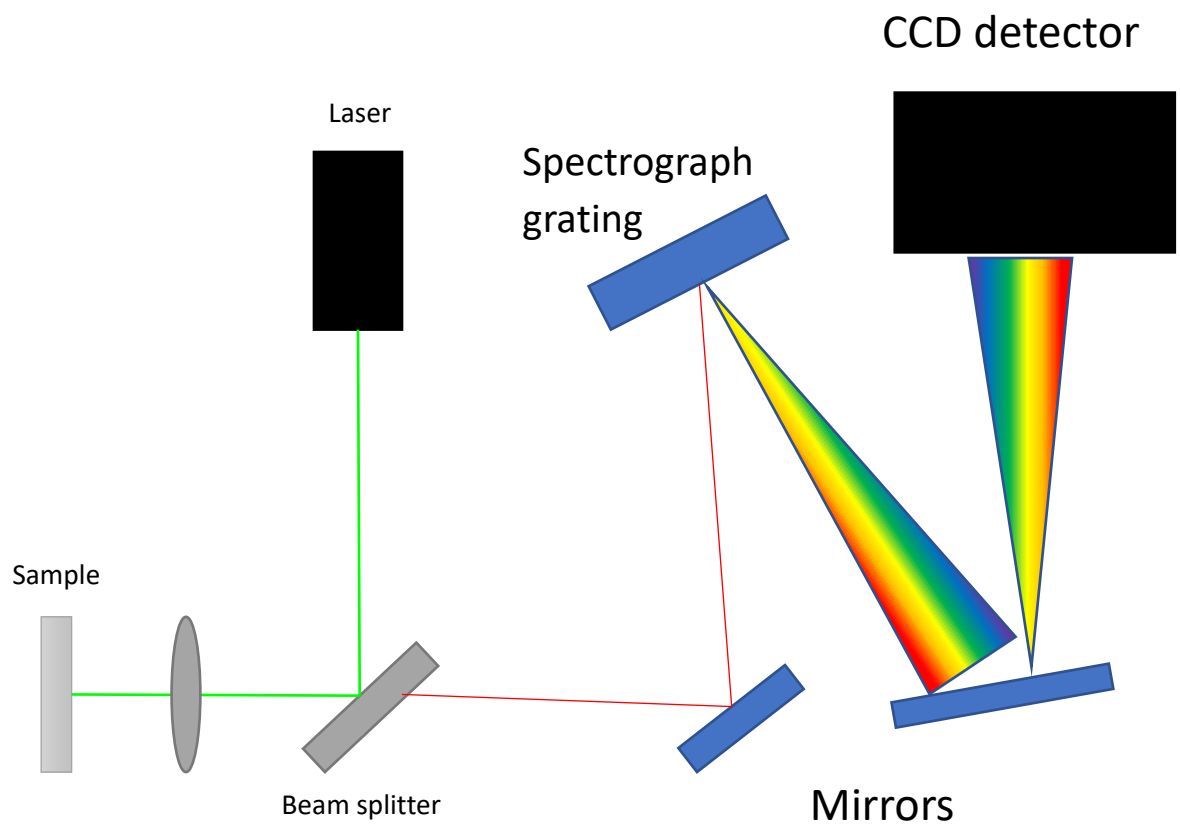

Figure 2.6- A diagram of a Raman spectrometer.[14]

The Raman spectrometer can have many different set ups, but every machine generally has the same key components. Every Raman spectrometer uses some sort of monochromatic excitation source, mainly a laser, to excite the sample. Laser stands for Light Amplification by Stimulated Emission of Radiation. In order for a laser to work there must be a population inversion where there are more molecules in the excited state instead of the usual distribution where most molecules occupy the ground state. When there is a population inversion the electrons in the excited state can undergo stimulated emission and emit photons of the same energy, which makes the light monochromatic. There are many advantages that a laser holds as an excitation source such as the fact that lasers are

monochromatic as previously mentioned, but lasers are also coherent, polarizable, and collimated.[15] Coherent light is light that is "in-step" and all the photons have the same energy, which allows the excitation source to be much more accurate than other sources that might not be coherent. Non-coherent light run through a monochromator could be very close to monochromatic, but some uncertainty would arise as the light would not all be the same. This is also why lasers producing monochromatic light is advantageous over polychromatic excitation sources as it allows for the changes in the sample to easily be known. Lasers are also collimated meaning that they have very little divergence and the beam that a laser emits is very thin and narrow. This can make working with lasers a bit dangerous as the beams are able to focus onto a very small area. Many different laser sources can be used for Raman spectroscopy throughout the light ranges of ultraviolet, visible, or even the near IR.[16] The most common Raman detector is the charge coupled device (CCD) detector which converts the scattered photons into an electrical signal on the computer. The range of this detector is said to end at about 1000 nm, but its detection can decrease rapidly after 800 nm so this must be taken into effect when choosing a laser. Another issue with lower wavelength lasers is that many molecules can undergo fluorescence, which drowns out the Raman signal. Several common types of lasers are listed below (Table 2.1) with their associated wavelengths.

Laser Type	Wavelength-λ
Argon	454.6 nm
HeNe	632.8 nm
Krypton	416 nm
Nitrogen	337.1 nm
CO_2	10.6 μm

Table 2.1- A table showing several common lasers that can be used in Raman spectroscopy and their corresponding wavelengths.[23]

Chapter 3: Theoretical Chemistry and Methods

3.1 Computational Chemistry

Theoretical chemistry is a branch of chemistry that uses calculations to solve certain problems. The applications of theoretical chemistry are enormous as some areas of chemistry, like astrochemistry, are not easy to study experimentally. Information on molecules that exist in conditions that are not replicable in the lab, molecules that are highly reactive, or molecules that have not even been synthesized yet can all be obtained by theoretical calculations with theoretical and computational chemistry. Theoretical chemistry also allows experimental chemists to have something to compare their data to, so if a molecule has never been studied before then theoretical chemistry can give an approximation on many different details. As technology has advanced and computers have gained exponentially more computing power the ability to use computational chemistry has grown and calculations can be increasingly accurate.

Computational chemistry at its core involves solving the Schrodinger equation (equation 3.1), which can be solved exactly for 1 electron systems.

$$\hat{H}\psi = E\psi \qquad \text{(eq. 3.1)}$$

In the Schrodinger equation E represents the total energy of the system while ψ represents the n-electron wave function that depends on both the identities and positions of the nuclei and the number of electrons in the system. $\hat{H}$ is the Hamiltonian operator, which is the total kinetic and potential energies of the system. The Hamiltonian can be broken down further as shown in equation 3.2 below.

$$\widehat{H} = -\frac{\hbar^2}{2m_e}\sum_i^{electrons}\nabla_i^2 - \frac{\hbar^2}{2}\sum_A^{nuclei}\frac{1}{M_A}\nabla_A^2 -$$

$$\frac{e^2}{4\pi\varepsilon_0}\sum_i^{electrons}\sum_A^{nuclei}\frac{Z_A}{r_{iA}} + \frac{e^2}{4\pi\varepsilon_0}\sum_i^{electrons}\sum_j^{electrons}\frac{1}{r_{ij}} +$$

$$\frac{e^2}{4\pi\varepsilon_0}\sum_A^{nuclei}\sum_B^{nuclei}\frac{Z_A Z_B}{R_{AB}} \quad \text{(eg 3.2)}^{21}$$

In this equation ħ is Planck's constant dived by 2π, m_e is the mass of an electron, ∇^2_i is the Laplace operator of particle i, M_A is the mass of nucleus A, ε_0 is the permittivity of free space, Z_A is the nuclear charge of A, r_{iA} is the distance between electron i and nucleus A, and R_{AB} is the distance between nuclei A and B.[21] A problem arises when there is more than 1 electron in a system, which is most atoms and molecules. Once 3 bodies are introduced there are too many variables in the Schrodinger equation to solve it exactly, so certain approximations can be made.

One of the earliest theories used in computational chemistry is the Hartree-Fock molecular orbital theory, which makes several approximations in order to solve the Schrodinger equation for a multielectron system. This theory yields the Hartree-Fock, or self-consistent field, method that can be used to solve the Schrodinger equation. One of the most important approximations that is made is called the Born-Oppenheimer approximation, which treats the motion of the nuclei and electrons separately and treats the nucleus, or nuclei, as stationary. The Hartree-Fock method also assumes that electrons are paired, which is one of its main problems as a model. This method approximates the wave function of the Schrodinger equation with a Slater determinant, from which a set of

functions can be derived that tell the Hatree-Fock equation. As mentioned previously this method is also called the self-consistent field (SCF) method because SCF theory is used to find the lowest energy structure in the Hartree-Fock method. Finally, an approximation called the linear combination of atomic orbitals (LCAO) translates the Hartree-Fock equations into more solvable forms that give the desired information.[22]

Other theories and methods have been produced that have lower computational costs and are usually more reliable than the Hartree-Fock method. One of these is density functional theory (DFT), another molecular orbital theory that uses functionals of electron density to determine the properties of a system. DFT and other such methods that have been created have advantages over the Hartree-Fock method, but they are still models and they do still have issues. DFT incorporates more of the characteristics of electrons in its calculations, which makes it more accurate, but phenomena like intermolecular interactions are still difficult to describe using DFT.[17] This shows that while new methods have been developed since the initial Hartree-Fock method computational chemistry is a field that is constantly evolving as theoretical chemists attempt to create more accurate models of the world that will create more accurate calculations.

3.2 Methods and Basis Sets

2 computational methods were used in this project along with 3 different basis sets for each method. The B3LYP and M06-2X methods were used along with the 6-

311+G(*d,p*), aug-cc-pVDZ, and aug-cc-VTZ basis sets. The B3LYP method, or Becke, 3 parameter, Lee-Yang-Parr method, is a hybrid functional, which is a functional in DFT that uses Hartree-Fock exchange correlation. While DFT methods are generally considered to be more reliable and lest computationally costly it is not quantum mechanical, so it must approximate exchange correlation. Hartee-Fock methods on the other hand can treat exchange correlation exactly, so the hybrid functionals seek to combine the best parts of both of these methods. The B3 portion of this method refers to 3 parameter exchange correlational functional, which mixes the Hartree-Fock exchange correlation into the DFT method. B3LYP is a popular method to begin calculations with as it is fairly quick and accurate, but other methods, such as MP2 or M06-2X, are generally used after B3LYP as they are more advanced methods that might take longer but yield better results.[18]

One of the methods that is considered to be more costly than B3LYP while yielding better results is M06-2X, which is a type of Minnesota functional. Minnesota functionals have been met with some controversy as some scientists claim that they produce biased data on transition metals while working well for main group elements, but since all the elements in this study are main group this method will work well for this study.[20] The M06-2X functional is a hybrid functional with 54% Hartree-Fock exchange.[19] The CCSD method is considered one of the best computational methods in computational chemistry as it sometimes even referred to as the "gold standard", but it is also very expensive and takes a long time for calculations to complete. Because of its high computational cost, it can be beneficial to try and find another method and basis set combination that yield similar results to the CCSD method. In previous Hammer lab studies with B-N dative bonds a combination that has been seen to give comparable results is the M06-2X/aug-cc-pVTZ

combination. Since this combination has been seen to yield similar results without being so costly it was considered that this combination should be used instead.

The first basis set used in this research was the 6-311+G(*d*,*p*) basis set. This is a split valence basis set, meaning that the valence orbitals are all represented by more than one basis function. This basis set is a lower quality basis set that is not very computationally costly, so it might not return the best results, but it serves as a good starting point for higher calculations. The next basis sets that were used are the aug-cc-pVDZ and VTZ basis sets. These sets are more reliable than the previous set, but they also cost more to run. The only difference in the VDZ and VTZ sets is that the VTZ set has a triple zeta while the VDZ only has a double zeta, which refers to the basis functions representing the valence orbitals. The VTZ basis set will therefore have a more advanced representation of the valence orbitals than the double zeta basis set. The aug on the front of the basis set denotes that diffuse functions have been added to the basis set.

Chapter 4: Results and Discussion

As previously stated, the purpose of this experiment was to examine the B-N bond in borane pyridine, examine how to vibrational modes of pyridine shift when a borane group is added onto the molecule, and examine how the vibrational modes of pyridine shift when the molecule interacts with water. Borane pyridine was examined with Raman spectroscopy experimentally and then with the Gaussian09 program theoretically. Normal pyridine was also examined in the same way. Finally, several mixes of pyridine and water were examined by Raman spectroscopy with a mole fraction of χ=0.9 to χ=0.3. The interaction of pyridine and water was also examined with the Gaussian09 program by modeling the interaction of 1 water molecule with pyridine. The experimental data for these scenarios was compared to theoretical data and the shift in the vibrational modes of pyridine in borane pyridine was compared to the shifts seen in the interaction between pyridine and water attributed to hydrogen bonding.

4.1 Pyridine

Experimental

A spectrum of pyridine was obtained with the Raman spectrometer using a 532 nm yag/nd laser. This spectrum was collected for the purposes of this experiment. The experimental spectrum is shown below in figure 4.1.1 and several relevant peaks are shown in figures after that.

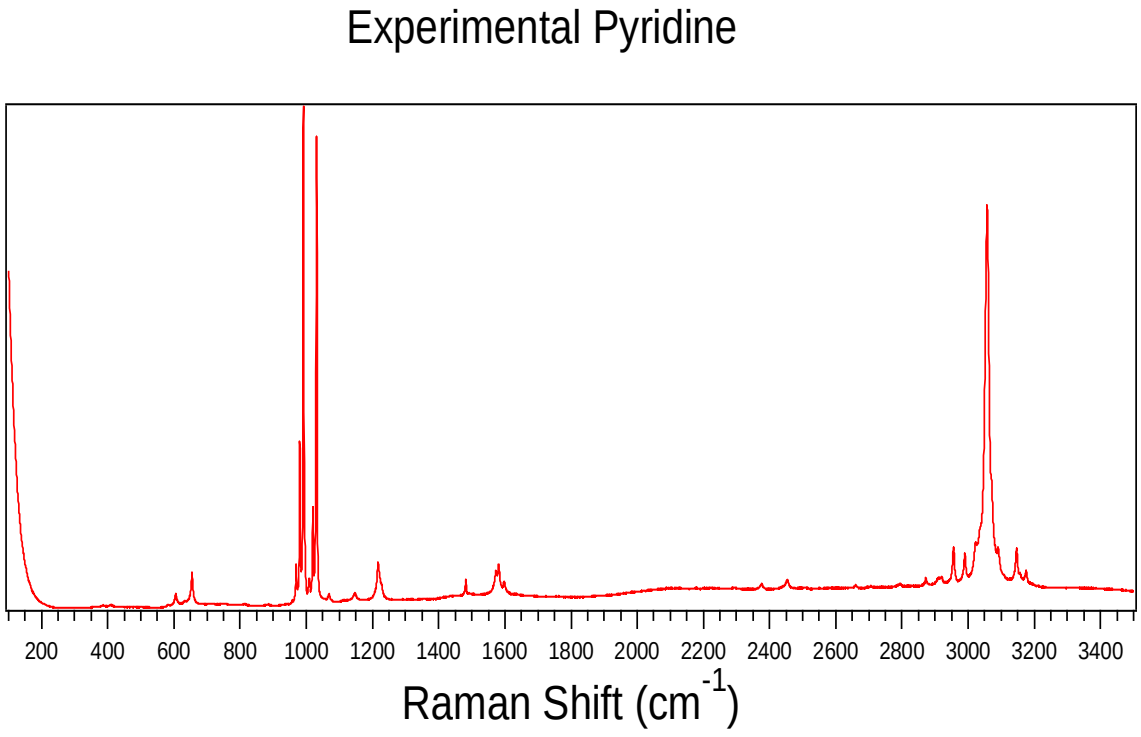

Figure 4.1.1- A graph of the experimental Raman spectrum of pyridine.

The three most important modes that will be examined for shifting due to interactions with the borane group or due to hydrogen bonding will be the peaks at 991, 1030, and 3057 cm^{-1}. Closer graphs of these modes are shown below in figures 4.1.2 and 4.1.3.

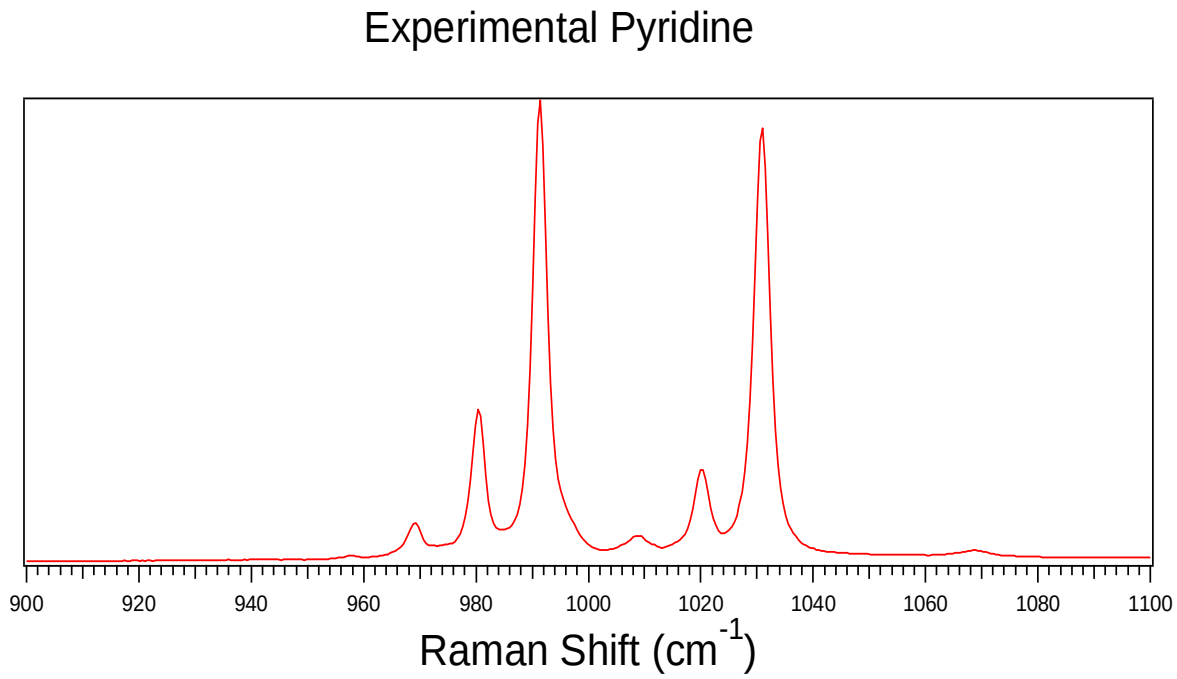

Figure 4.1.2- A figure showing the modes at 991 and 1030 cm^{-1}. The vibrational mode at 991 cm^{-1} was found to be a ring breathing mode while the mode at 1030 was found to be a ring stretching mode.

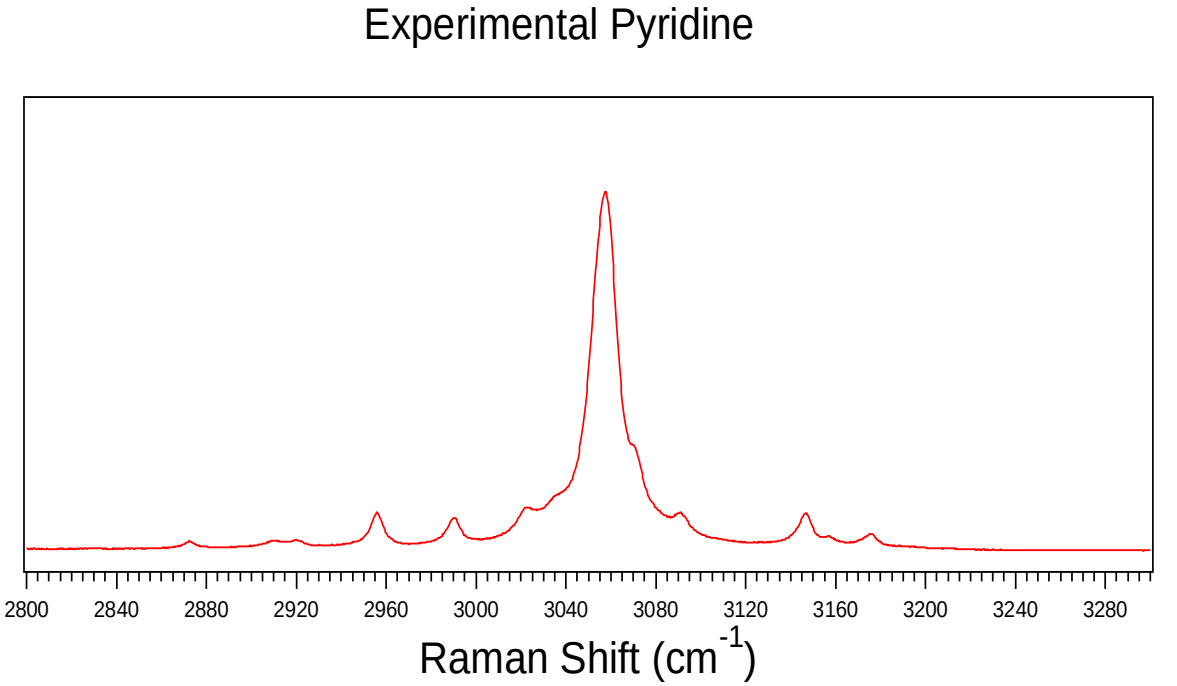

Figure 4.1.3- A graph showing the vibrational mode at 3057 cm^{-1}. This mode was found to be a C-H stretching mode.

Theory

The theoretical spectra of pyridine were found using the Gaussian09 program and as shown previously in the paper the methods used were B3LYP and M06-2X while the basis sets used were the 6-311+G(*d*,*p*), aug-cc-pVDZ, and aug-cc-pVTZ basis sets. The theoretical spectra of pyridine are shown below in figure 4.1.4 and closer examinations of the important modes are shown in figures 4.1.5 and 4.1.6. All theoretical calculations were scaled due to their respective methods and basis sets and the scaling factors used will be discussed later.

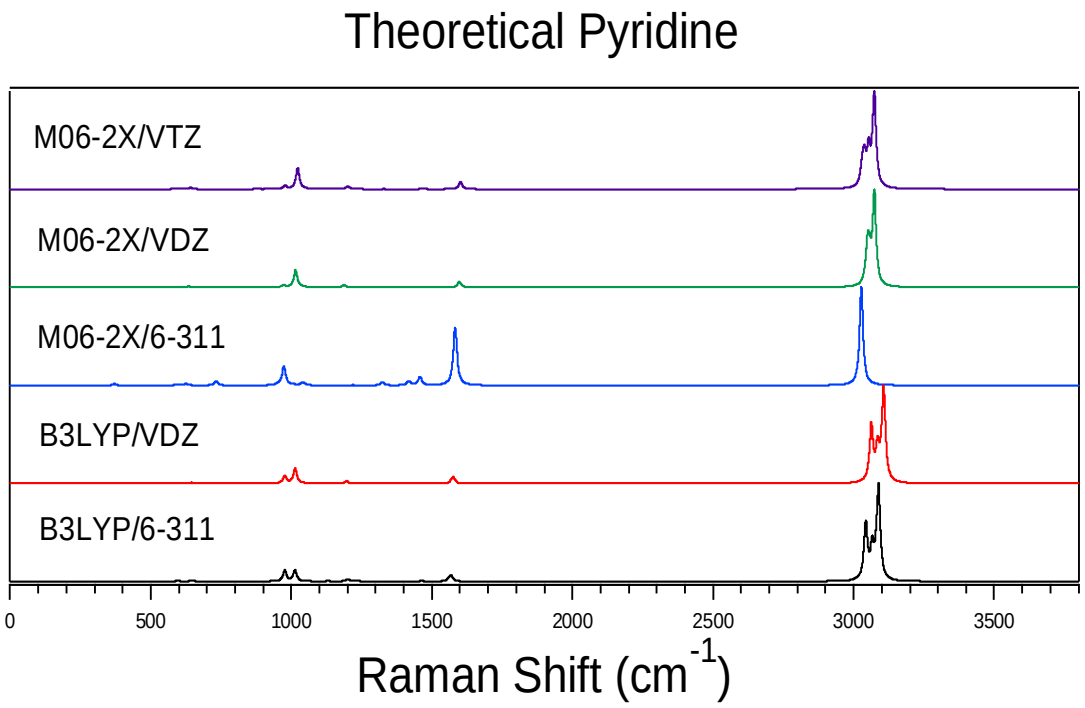

Figure 4.1.4- A figure showing the theoretical spectra obtained from the various combinations of methods and basis sets.

As it is difficult to see the peaks for all 5 combinations on one graph the close-up graphs for the theoretical section will be split into a graph with the M06-2X plots, figures 4.1.5 and 4.1.7, and a graph with the B3LYP plots, figures 4.1.6 and 4.1.8. The experimental plot of pyridine will also be included so that the plots can be compared later.

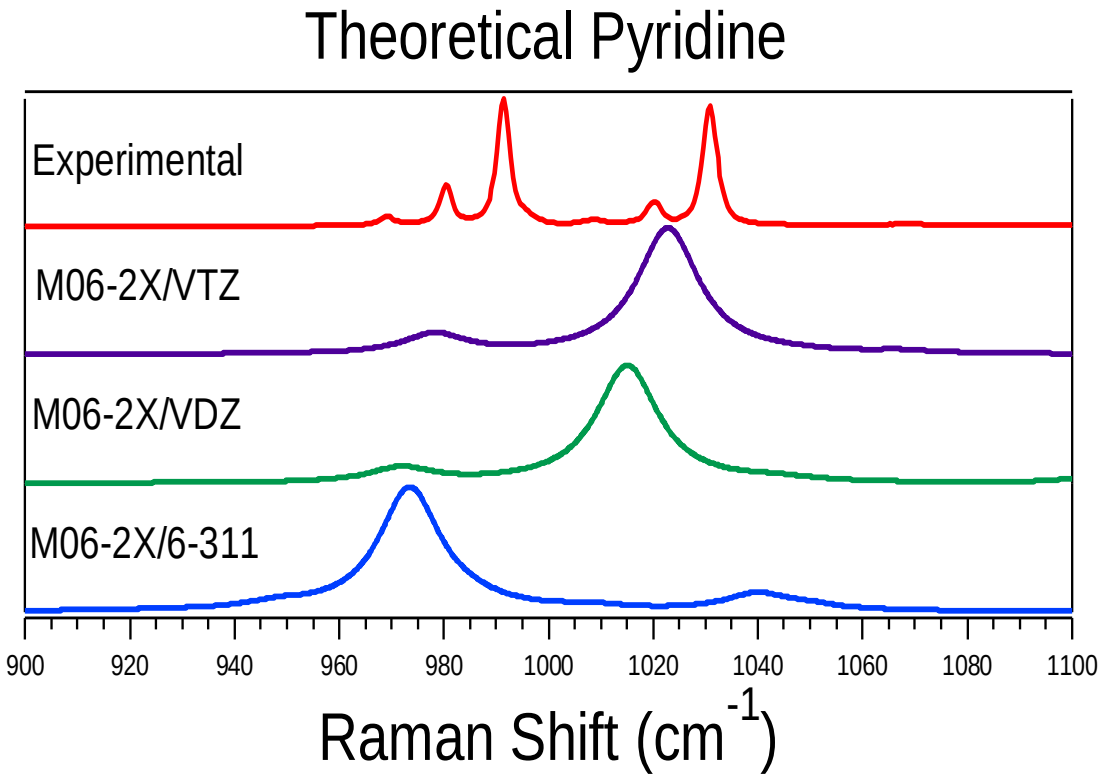

Figure 4.1.5- A graph showing the first 2 modes of note of pyridine for the calculations with a M06-2X method.

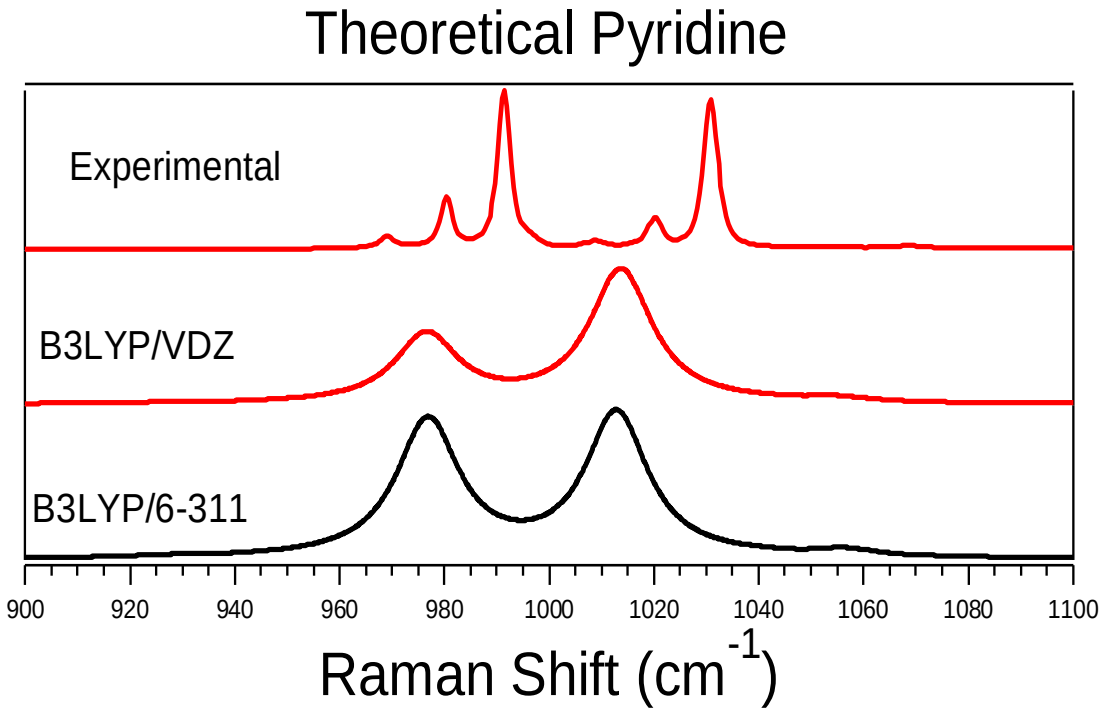

Figure 4.1.6- A graph showing the first 2 modes of note of pyridine for the calculations with a B3LYP method.

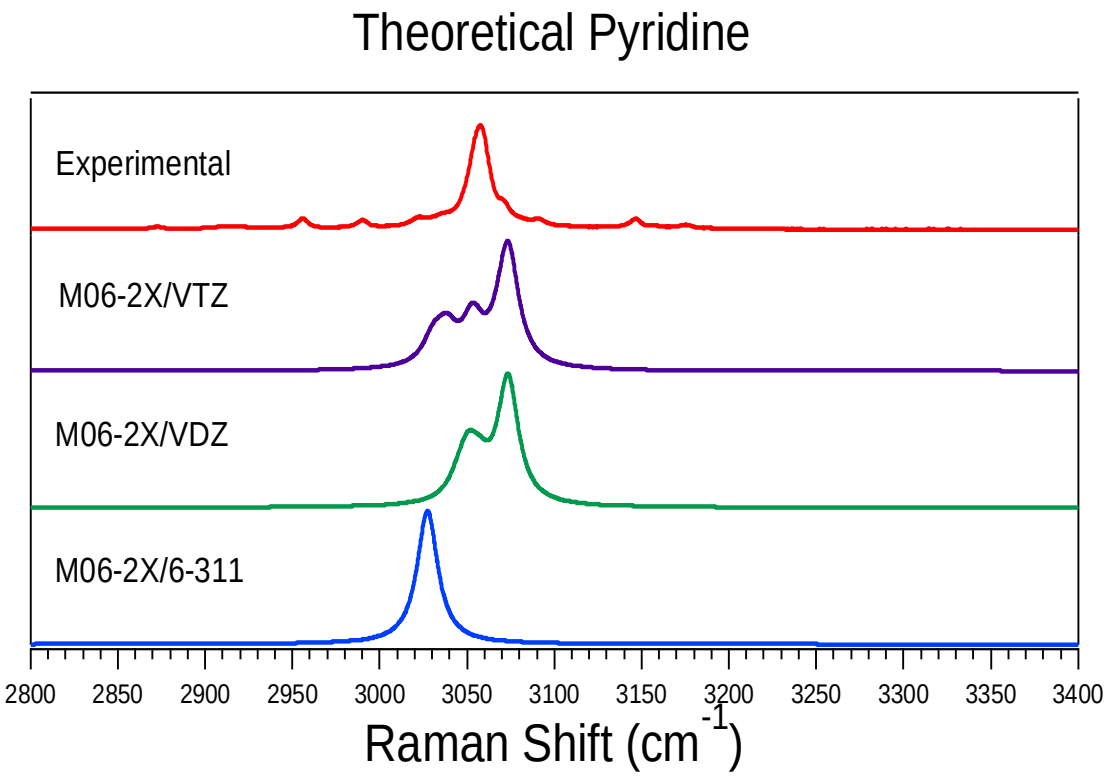

Figure 4.1.7-A graph showing the final mode for the calculations with a M06-2X method.

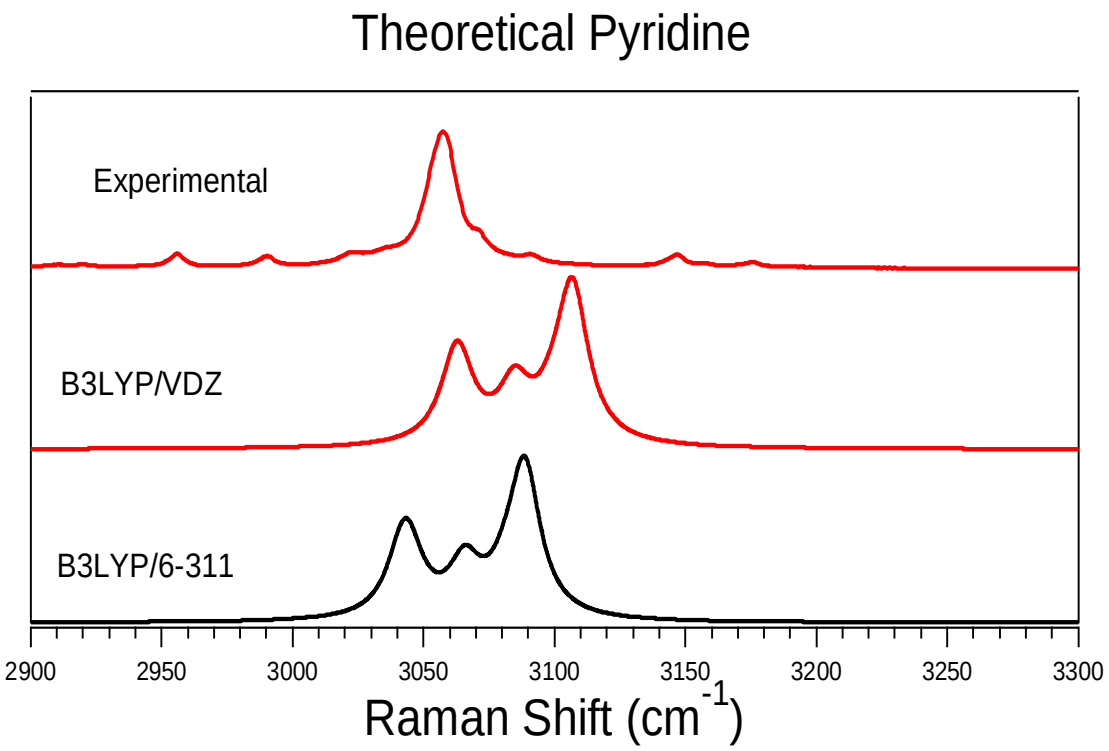

Figure 4.1.8-A graph showing the final mode for the calculations with a B3LYP method.

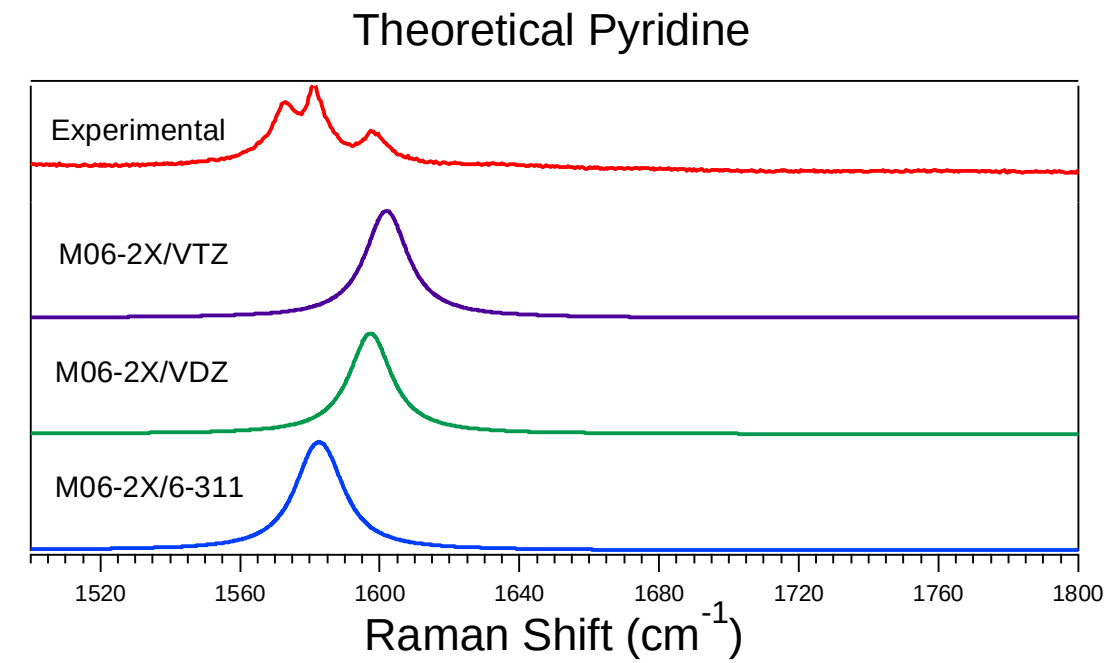

Figure 4.1.9-A graph showing the ring stretching mode for the calculations with a M06-2X method.

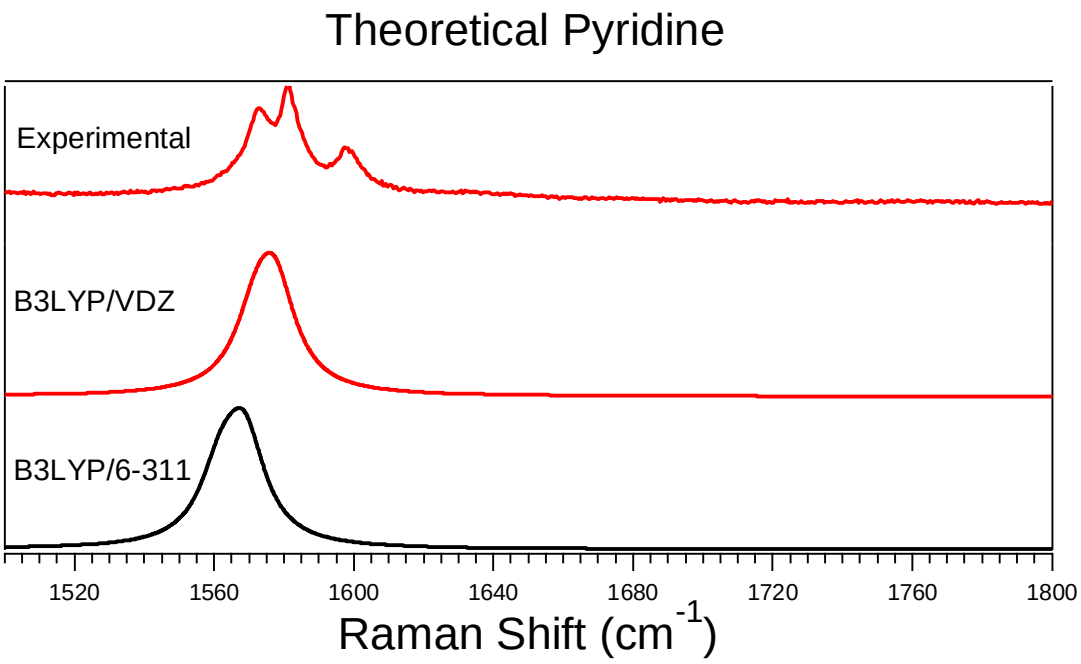

Figure 4.1.10-A graph showing the ring stretching mode for the calculations with a B3LYP method.

4.2 Borane Pyridine

Experimental

A 532 nm argon laser was used to find the Raman spectra of all the compounds in this study. The experimental data was obtained through the LabSpec program and was then transferred into the Igor graphing program. The experimental spectrum was collected for the purposes of this experiment and is shown below in figure 4.2.1. Close-up graphs with pyridine as a reference are shown below as well.

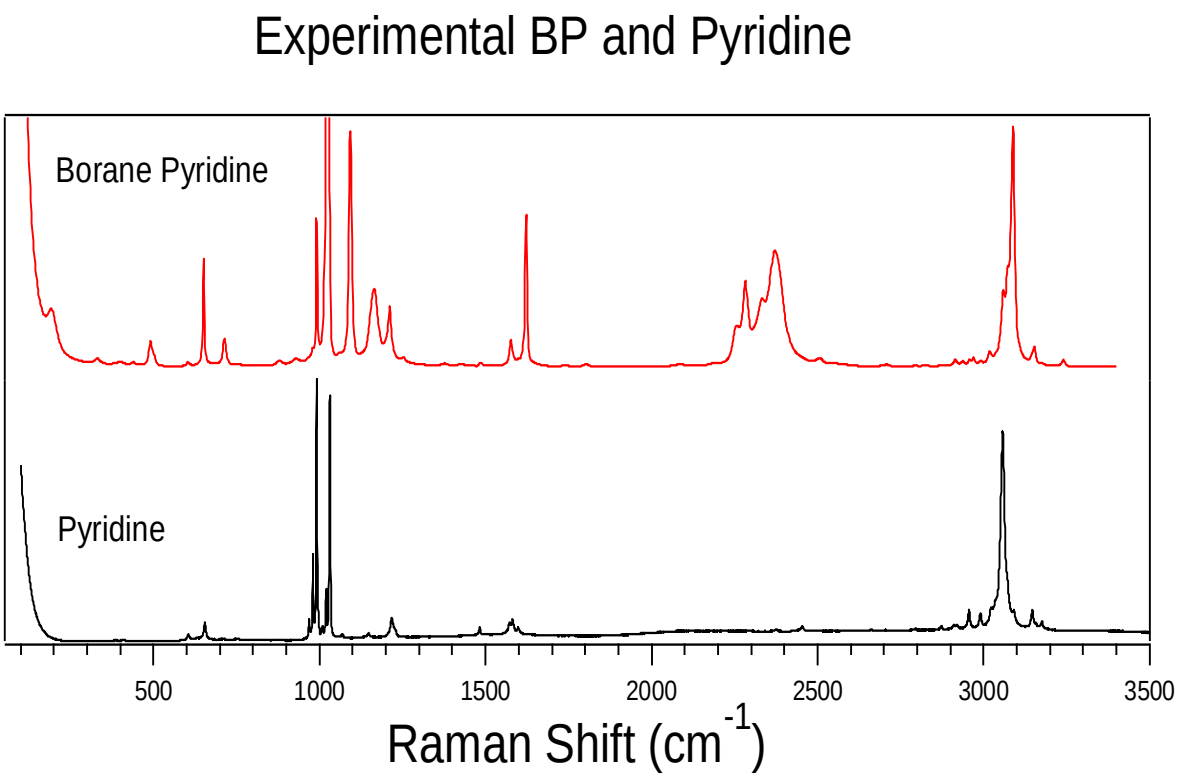

Figure 4.2.1- A graph showing experimental spectra of borane pyridine and pyridine for comparison.

Two close-up graphs of borane pyridine with pyridine are shown below in figures 4.2.2 and 4.2.3 and one close up graph of just borane pyridine in figure 4.2.4 is shown to show the B-H stretches in the plot.

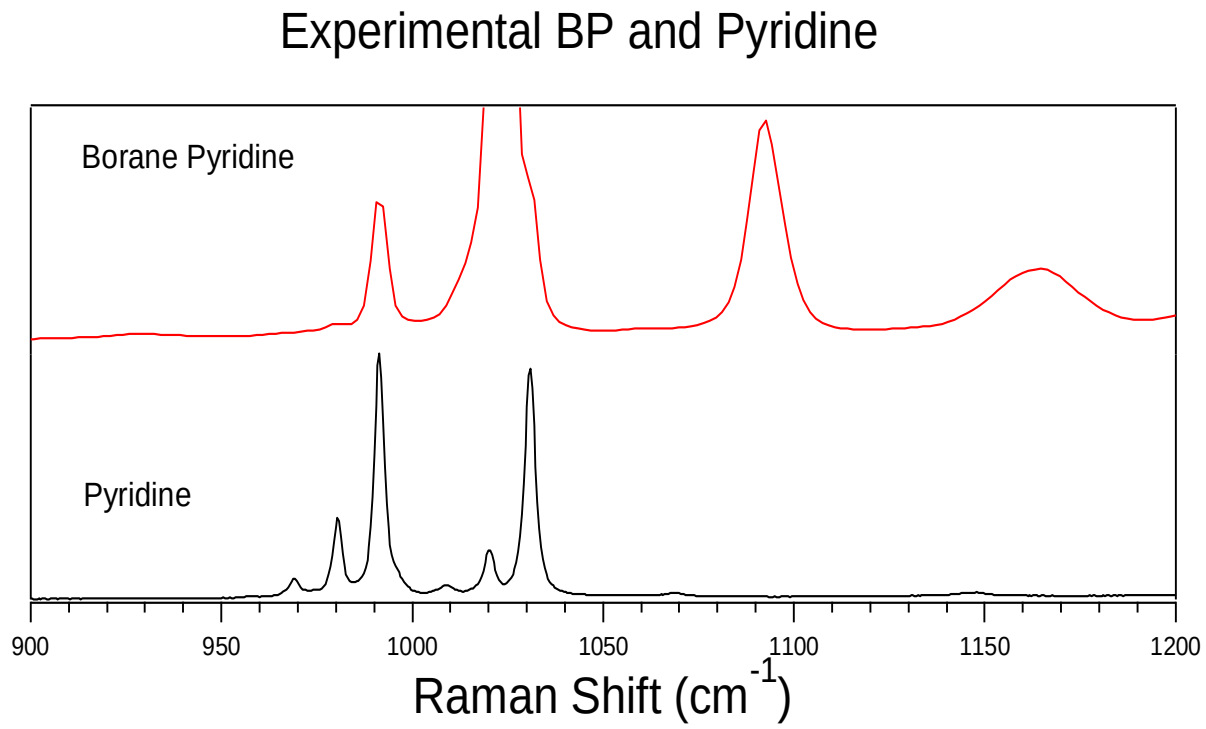

Figure 4.2.2- A graph showing the experimental borane pyridine spectrum compared with the pyridine spectrum. The two pyridine modes at 991 and 1030 cm^{-1} are shifted to 1023 and 1092 cm^{-1} in borane pyridine.

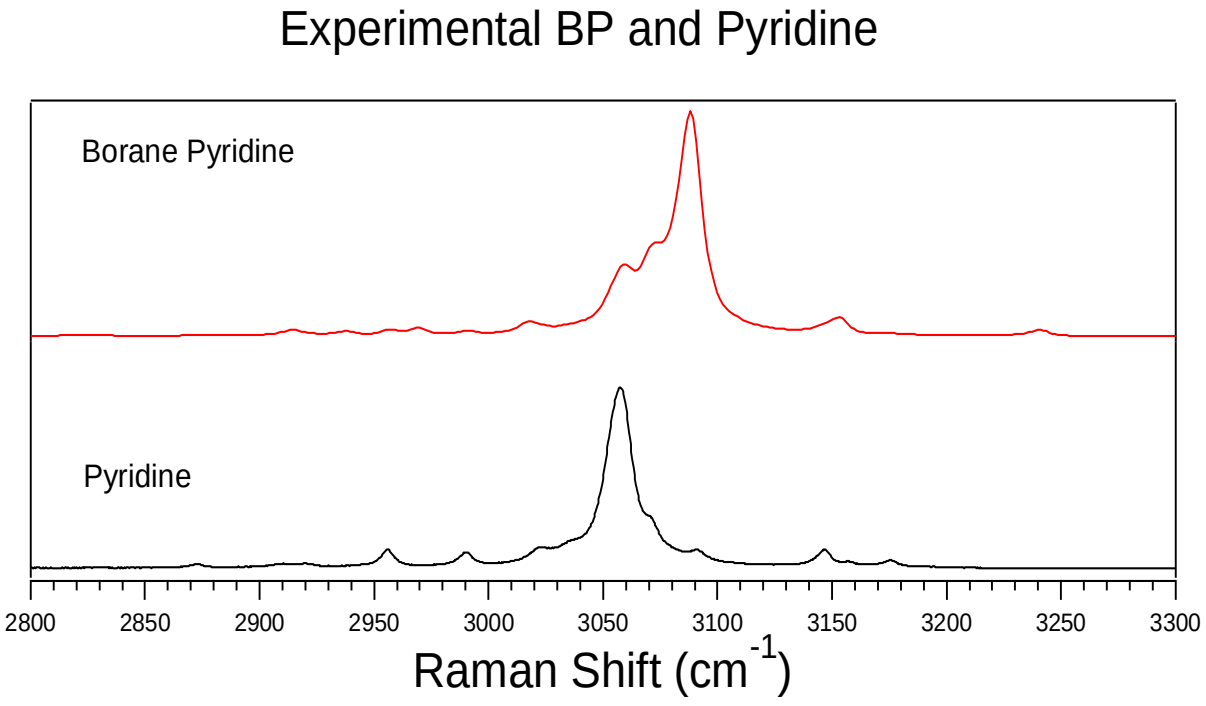

Figure 4.2.3- A graph showing the third important vibrational mode of experimental pyridine and borane pyridine. The pyridine mode at 3057 cm^{-1} has shifted to 3088 cm^{-1}.

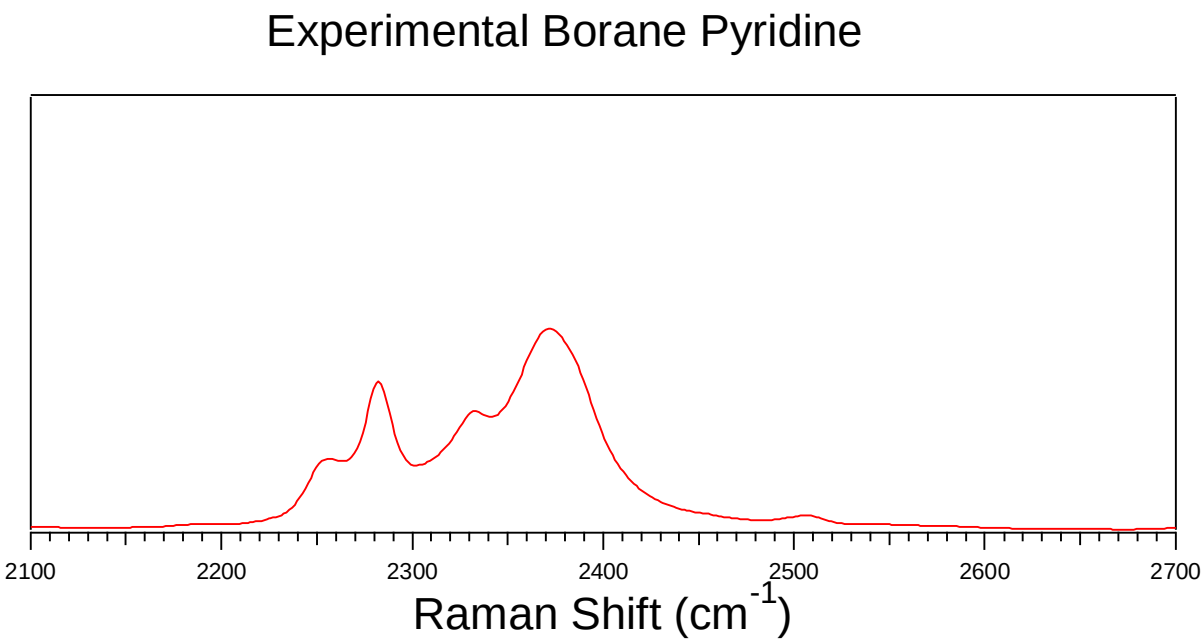

Figure 4.2.4- A figure showing the experimental B-H modes of borane pyridine. The important mode of these stretches is at 2370 cm^{-1} with another stretch at 2240 cm^{-1}. Pyridine obviously does not have B-H stretches so there was no shift in this plot.

Theory

The theoretical spectra of borane pyridine were found using the Gaussian09 program and as shown previously in the paper the methods used were B3LYP and M06-2X while the basis sets used were the 6-311+g(d,p), aug-cc-pVDZ, and aug-cc-pVTZ basis sets. The theoretical spectra of borane pyridine are shown below in figure 4.2.5 and closer examinations of the important modes are shown in figures 4.2.6-4.2.11.

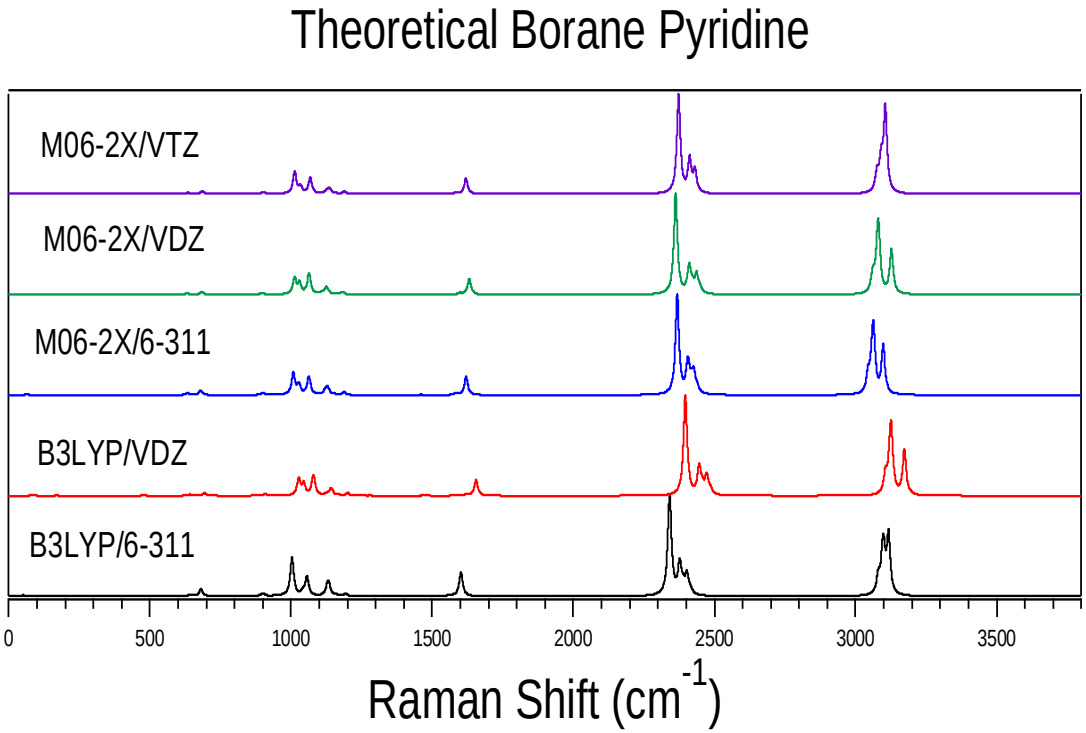

Figure 4.2.5- The theoretical spectra of Borane Pyridine obtained from the various basis sets and methods.

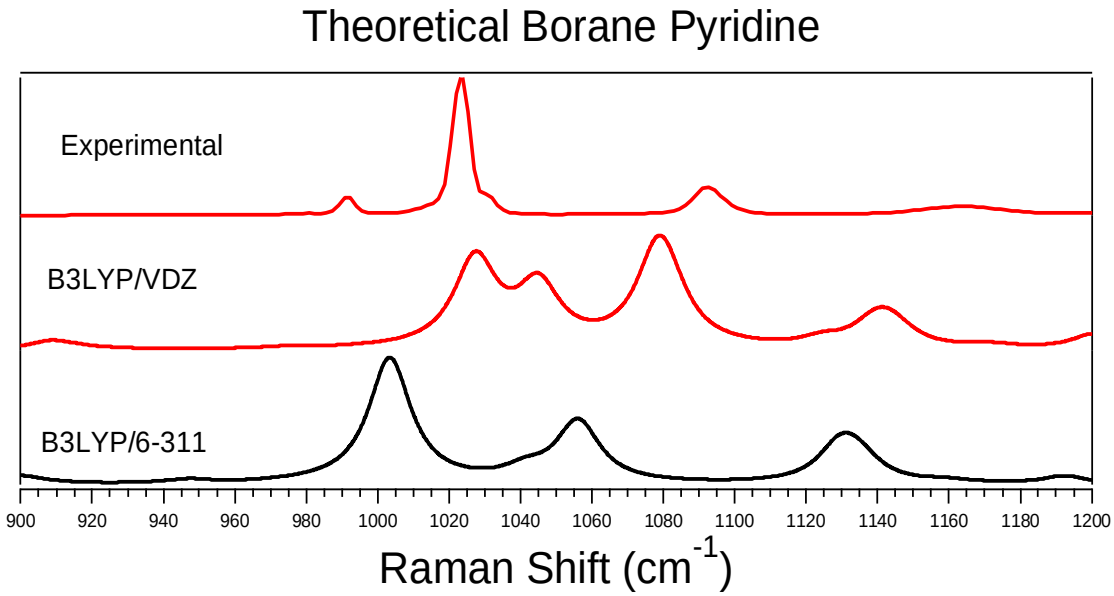

Figure 4.2.6- A figure showing the first two modes for calculations with a B3LYP method. The graph also shows the experimental plot for comparison.

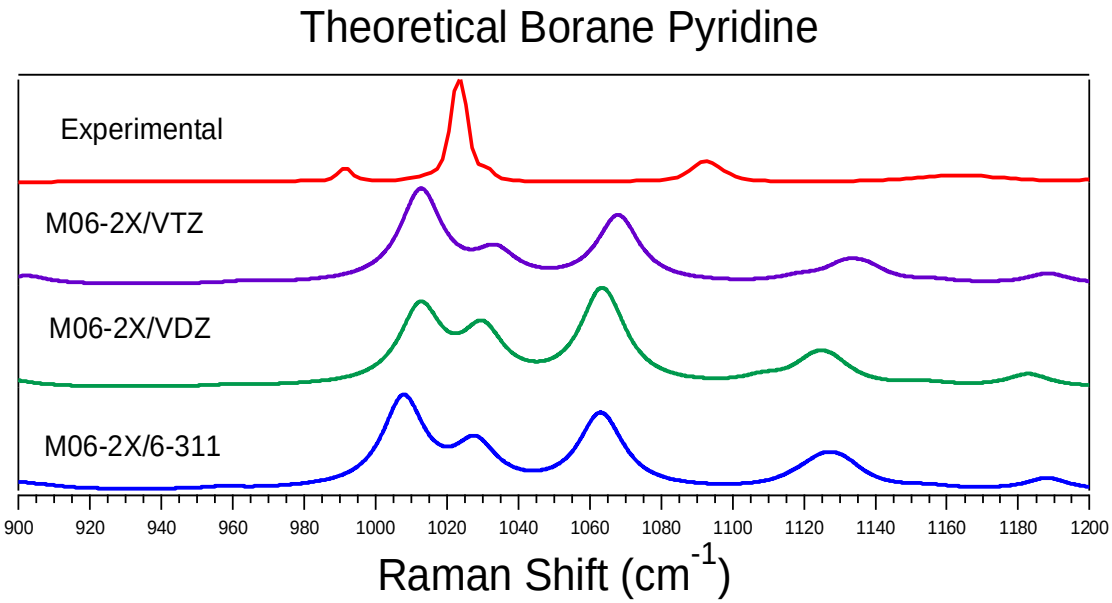

Figure 4.2.7- A figure showing the first two modes for calculations with a M06-2X method. The graph also shows the experimental plot for comparison.

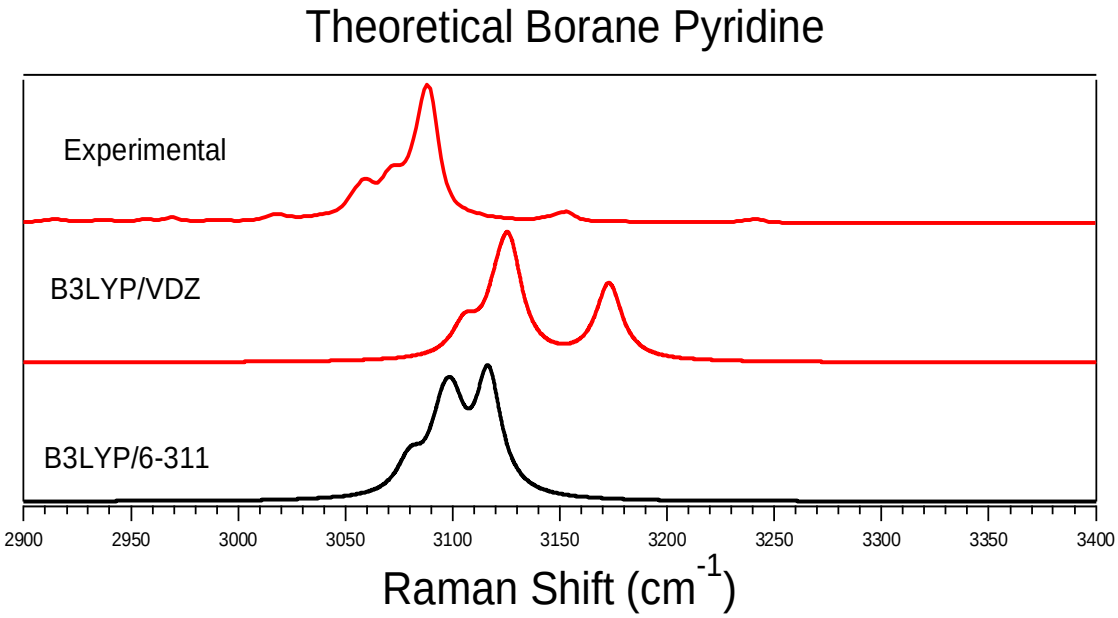

Figure 4.2.8- A figure showing the last mode for calculations with a B3LYP method. The graph also shows the experimental plot for comparison.

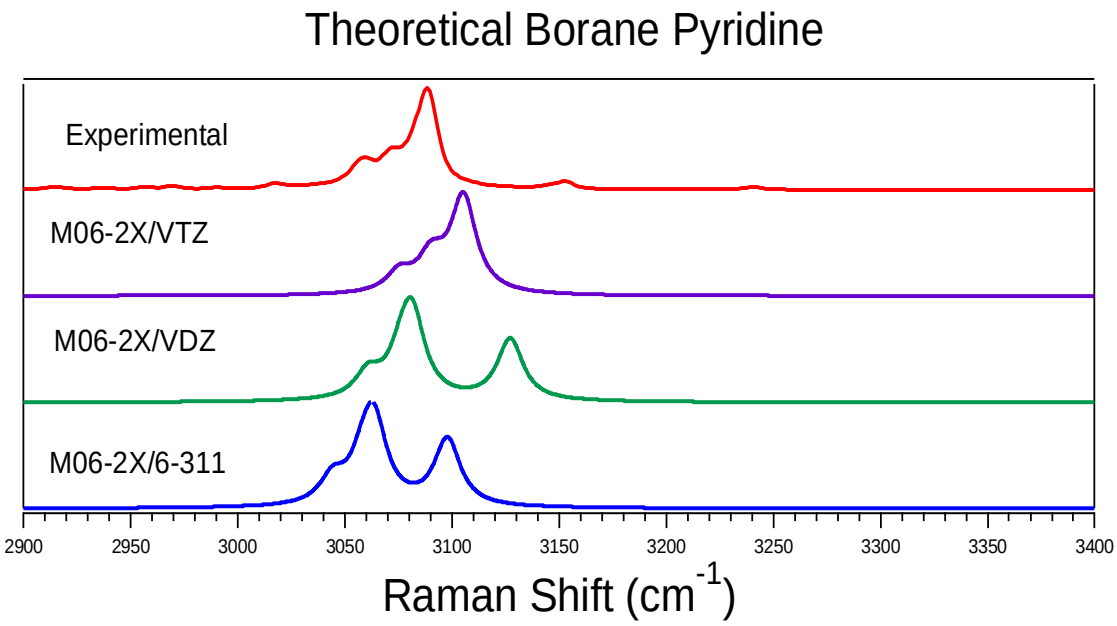

Figure 4.2.9- A figure showing the last mode for calculations with a M06-2X method. The graph also shows the experimental plot for comparison.

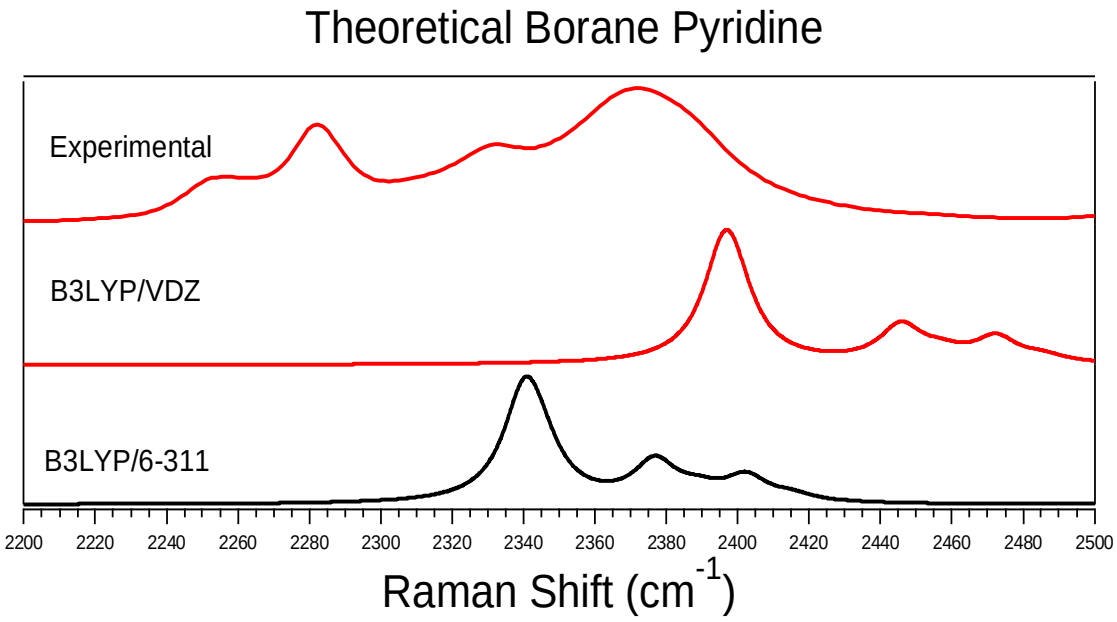

Figure 4.2.10- A Graph showing the B-H stretching modes for the B3LYP method calculations. The plot also shows the experimental graph for comparison.

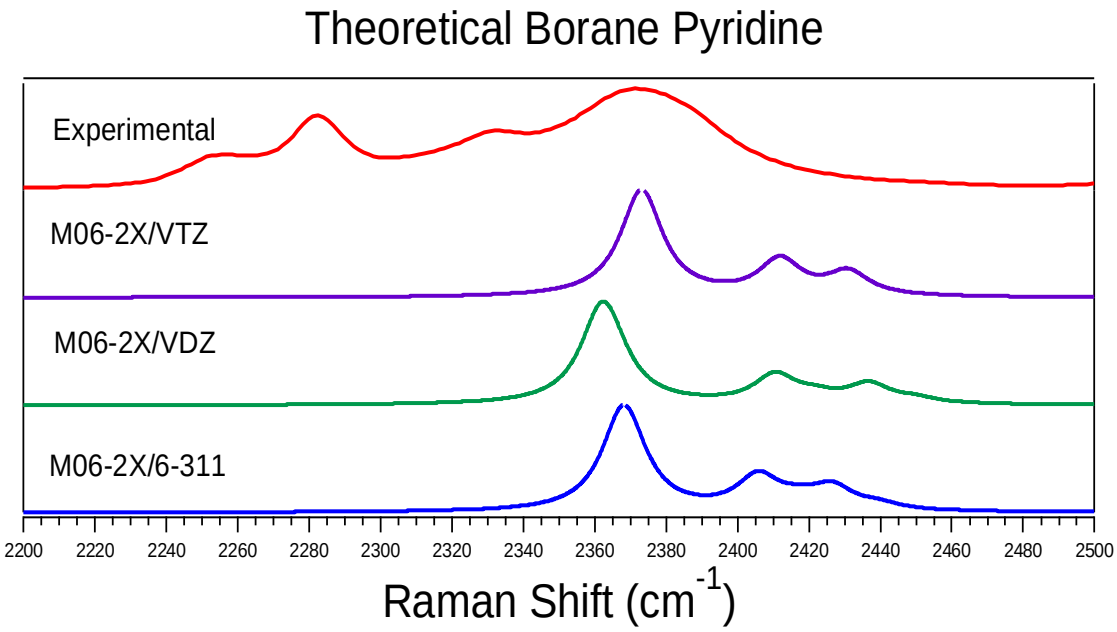

Figure 4.2.11- A Graph showing the B-H stretching modes for the M06-2X method calculations. The plot also shows the experimental graph for comparison.

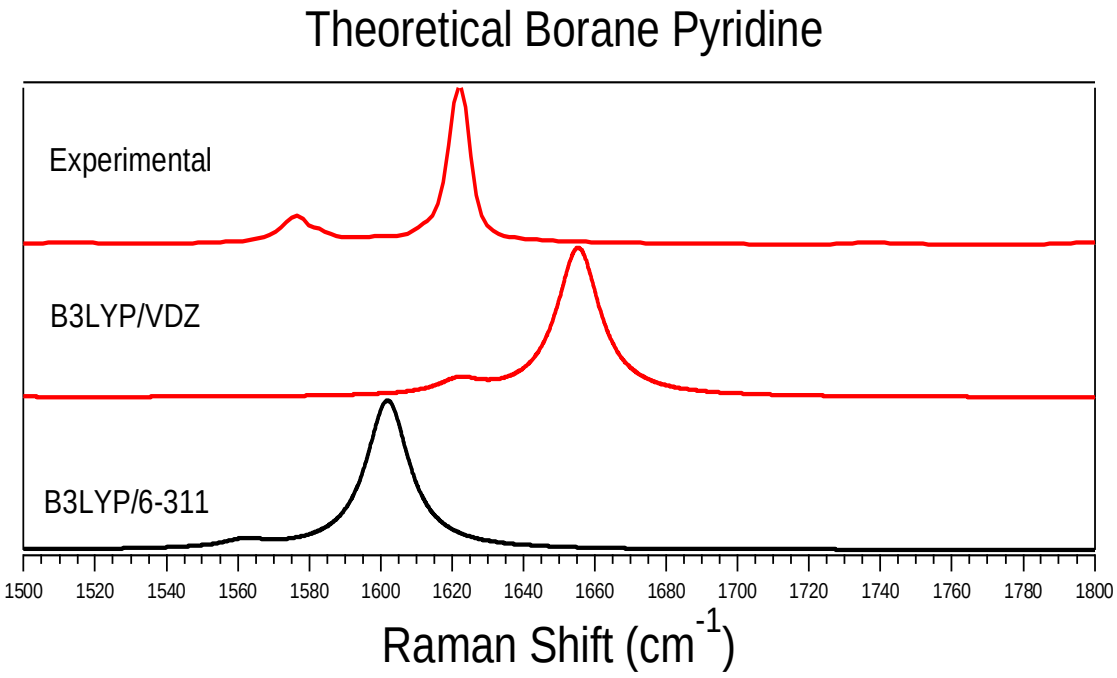

Figure 4.2.12- A Graph showing the ring stretching mode for the B3LYP method calculations. The plot also shows the experimental graph for comparison.

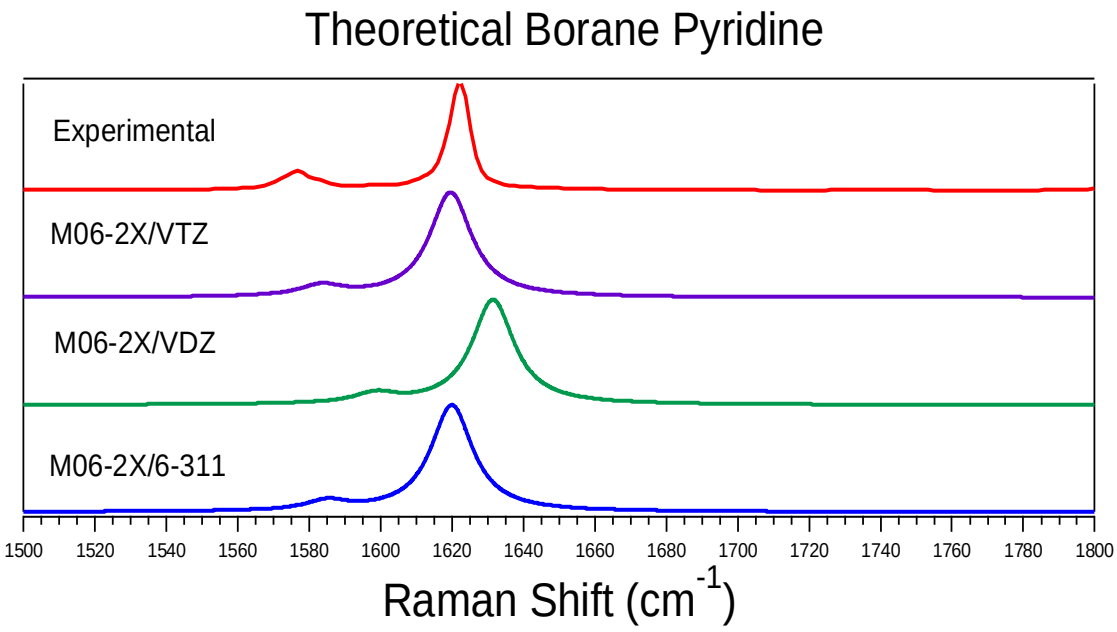

Figure 4.2.12- A Graph showing the ring stretching mode for the M06-2X method calculations. The plot also shows the experimental graph for comparison.

4.3 Pyridine and Water

Experimental

Pyridine and water were mixed in mole fractions ranging from χ=0.3 to χ=0.9 and then the Raman spectra of these mixtures were taken. These spectra were obtained for the purpose of this experiment. A graph of these spectra is shown below in figure 4.3.1 and close-up graphs of pyridines modes are shown after this figure with the spectrum of pure pyridine for later comparison.

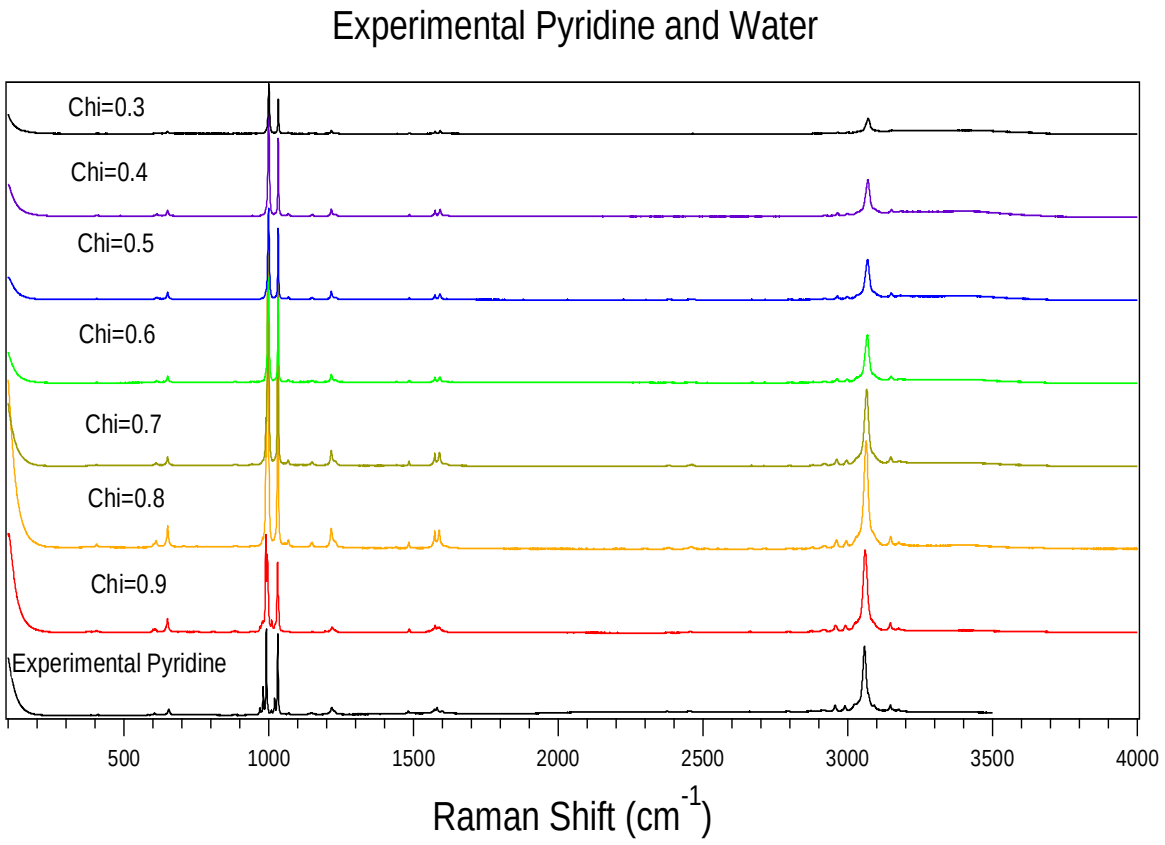

Figure 4.3.1- A figure showing the 7 pyridine and water samples that were examined with Raman spectroscopy along with the spectrum for pure pyridine.

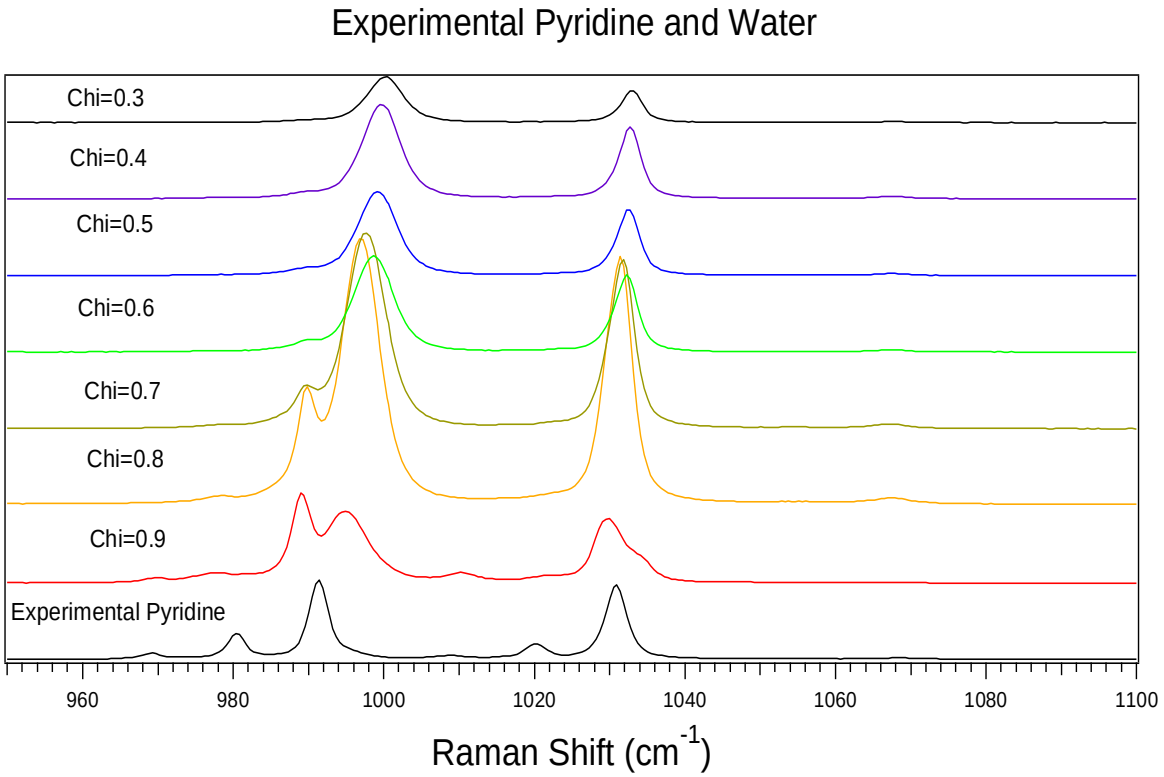

Figure 4.3.2- A figure showing the first two modes of pyridine and water with the plot of just pyridine as a comparison. The modes at 991 and 1030 cm^{-1} have been shifted to 1000 and 1033 cm^{-1} in χ=0.3.

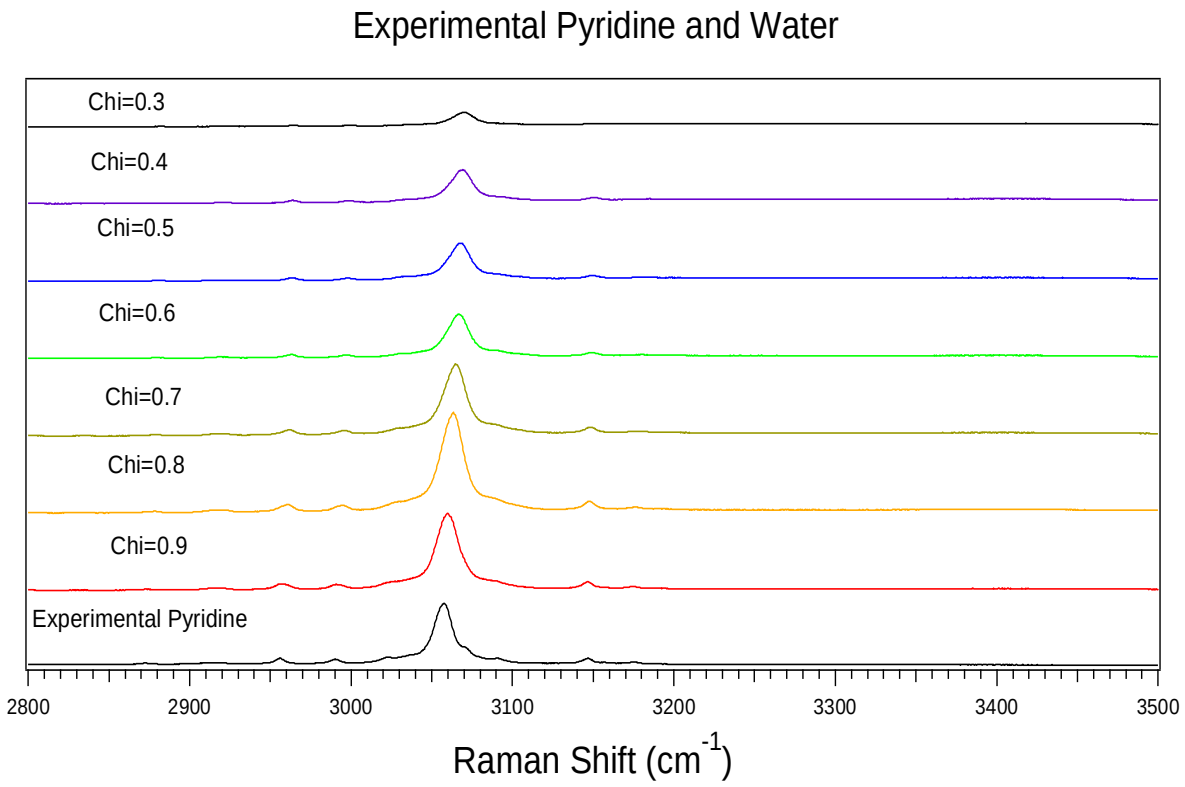

Figure 4.3.3- A graph showing the last mode of pyridine compared with the pyridine and water samples. The mode at 3057 cm^{-1} has been shifted to 3070 cm^{-1}.

To show the effects of hydrogen bonding on pyridine graphs of pyridine and water at mole fractions of 0.9,0.5, and 0.3 are shown below so that the mode associated with hydrogen bonding can be seen.

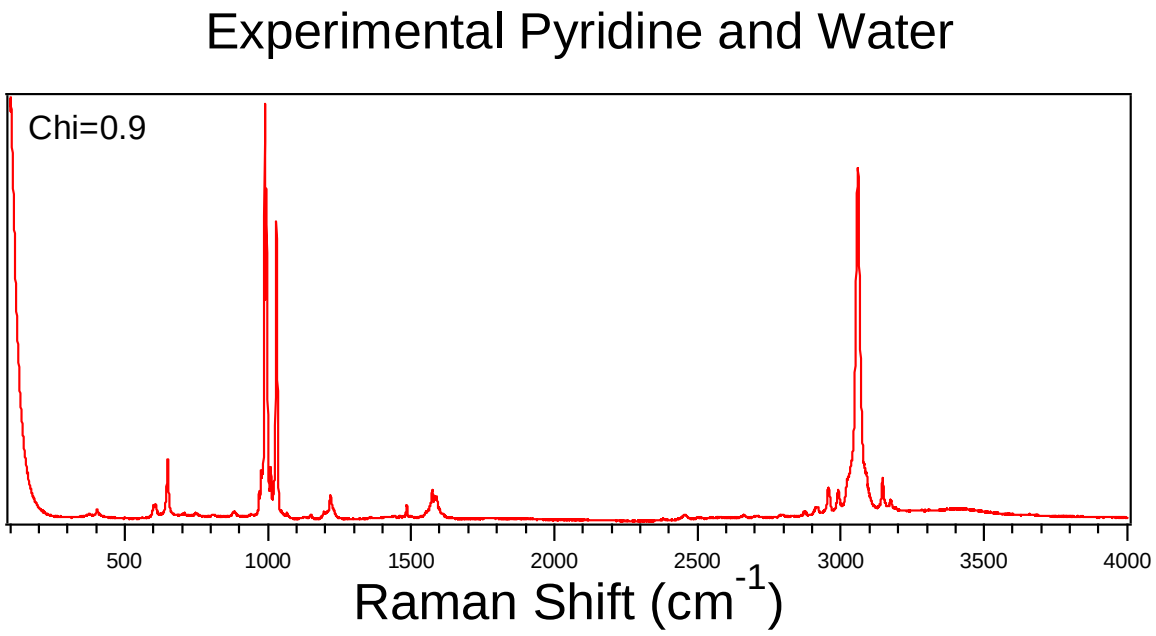

Figure 4.3.4- A plot of just pyridine and water at a mole fraction of χ=0.9.

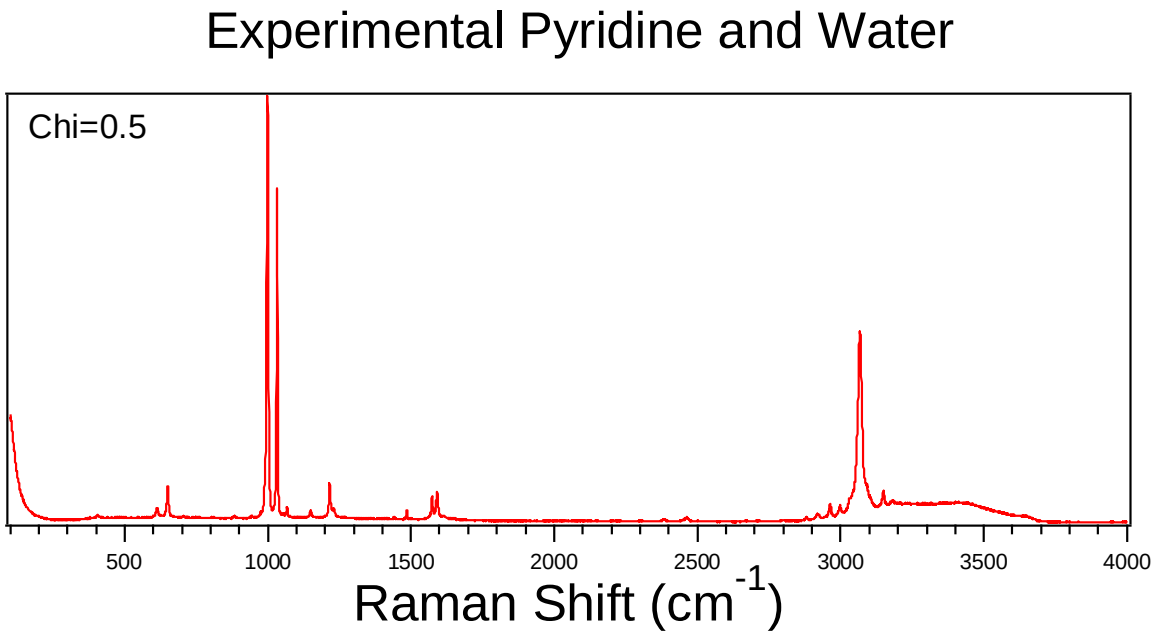

Figure 4.3.5- A plot of just pyridine and water at a mole fraction of χ=0.5.

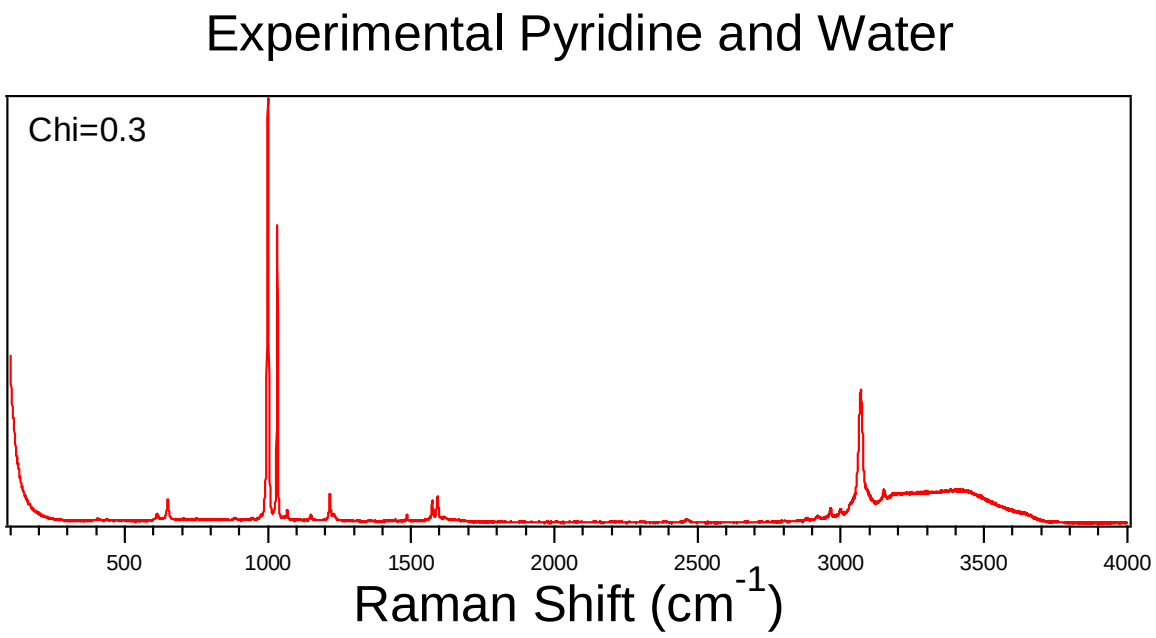

Figure 4.3.6- A plot of just pyridine and water at a mole fraction of χ=0.3.

Theory

The theoretical spectrum of pyridine and water was found using the Gaussian09 program. The structure was first optimized so that the correct position of the water molecule would be known. The method used was M06-2X while the basis set used was the aug-cc-pVTZ basis set. The theoretical spectrum of pyridine and water is shown below in figure 4.3.7 with the experimental plot of pyridine and water at χ=0.5 for comparison. Closer examinations of the important modes are shown in figures 4.3.8-4.3.11.

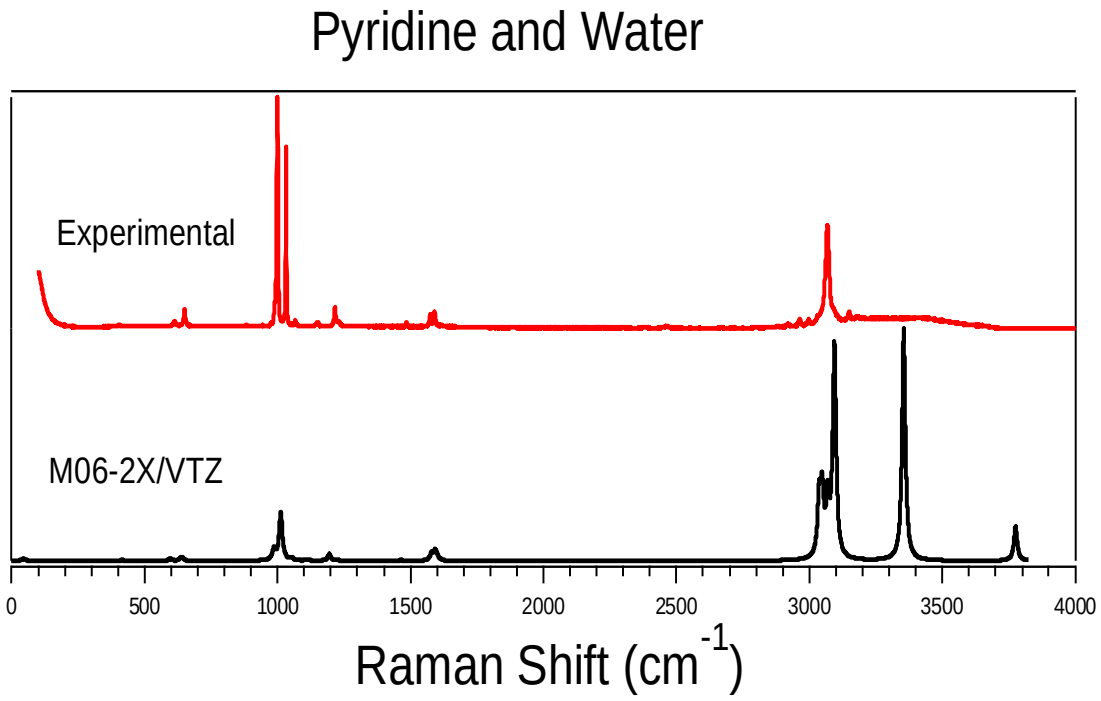

Figure 4.3.7- A figure comparing the vibrational modes of theoretical and experimental pyridine and water.

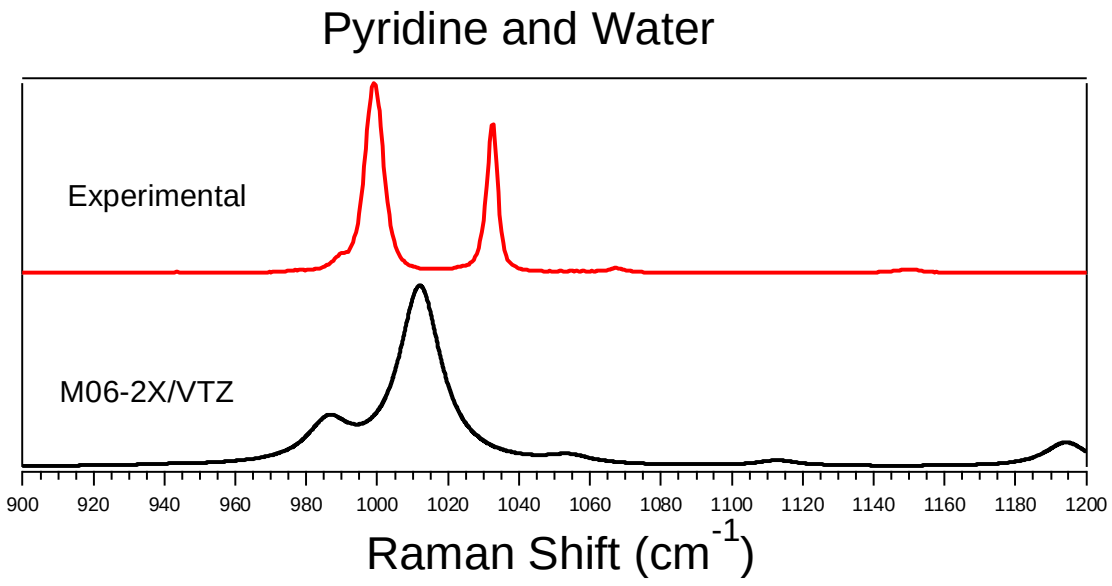

Figure 4.3.8- A figure showing the first two modes of pyridine and water with a M06-2X method and an aug-cc-pVTZ basis set.

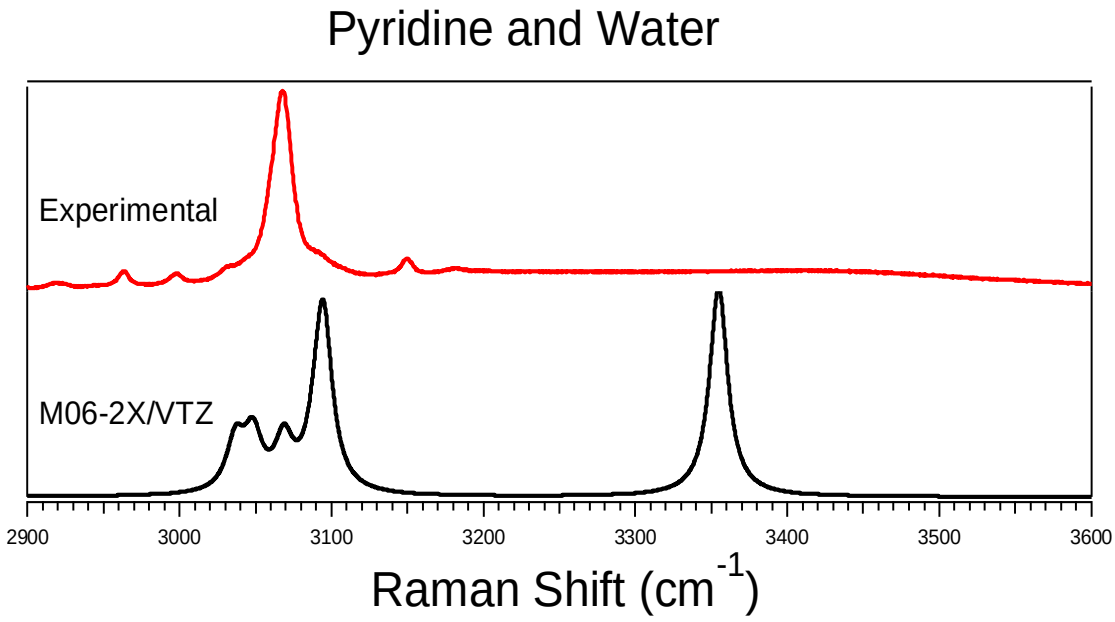

Figure 4.3.9- A figure showing the last mode of pyridine and water with a M06-2X method and an aug-cc-pVTZ basis set.

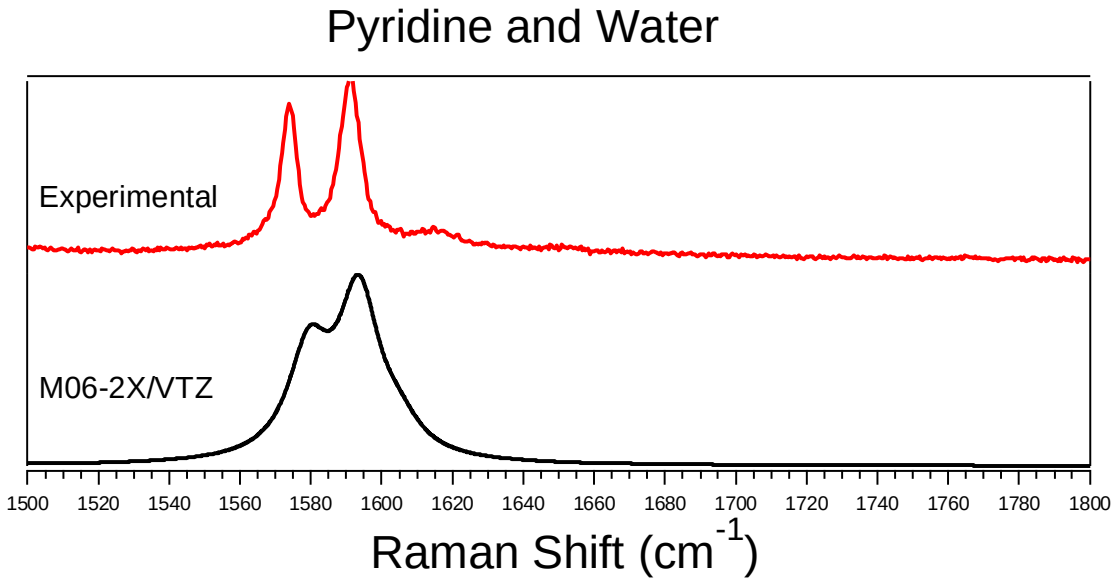

Figure 4.3.9- A figure showing the ring stretching mode of pyridine and water with a M06-2X method and an aug-cc-pVTZ basis set.

For the sake of clarity all the important vibrational modes from all the experimental and theoretical spectra are included in a table below.

Exp Pyridine	Theory Pyridine M06-2X/VTZ	Peak Type
991 (cm^{-1})	978 (cm^{-1})	C-H ring stretch
1030 (cm^{-1})	1023 (cm^{-1})	Ring "Breathing"
1580 (cm^{-1})	1603 (cm^{-1})	Ring Stretching
3057 (cm^{-1})	3074 (cm^{-1})	C-H stretch
Exp Borane Pyridine	Theory Borane Pyridine M062X/VTZ	Peak Type
719 (cm^{-1})	687 (cm^{-1})	B-N stretch
1023 (cm^{-1})	1014 (cm^{-1})	C-H ring stretch
1092 (cm^{-1})	1068 (cm^{-1})	Ring "Breathing"
1622 (cm^{-1})	1620 (cm^{-1})	Ring Stretching
2370 (cm^{-1})	2374 (cm^{-1})	B-H stretch
3088 (cm^{-1})	3106 (cm^{-1})	C-H stretch
Exp Pyridine & Water	Theory Pyridine & Water M06-2X/VTZ	Peak type
1000 (cm^{-1})	1000 (cm^{-1})	C-H ring stretch
1033 (cm^{-1})	1032 (cm^{-1})	Ring "Breathing"
1592 (cm^{-1})	1592 (cm^{-1})	Ring Stretching
3070 (cm^{-1})	3069 (cm^{-1})	C-H stretch

Table 4.3.1- A table showing all the important vibrational modes from the results section in one place for easy comparison.

Another table is also included below with all the scaling factors used for the theoretical calculations.

Method/Basis set	Scaling factor
B3LYP/6-311+G(*d,p*) (6-311+G(*3df,2p*))	.967
B3LYP/aug-cc-pVDZ	.970
M06-2X/6-311+G(*d,p*) (6-31G(*2df,p)*)	.952
M062X/ aug-cc-pVDZ (aug-cc-pVTZ)	.956
M062X/ aug-cc-pVTZ	.956

Table 4.3.2- A table showing the scaling factors for the methods and basis sets used. The basis sets in parentheses are the basis sets that the scaling factors were taken from if there was not a scaling factor for the specific combination. There was not a scaling factor for B3LYP/6-311+G(*d,p*) so the scaling factor for B3LYP/6-311+G(*3df,2p*) was used since this basis set is fairly close. There were also not scaling factors for M06-2X/6-311+G(*d,p*) or M062X/ aug-cc-pVDZ so scaling factors from close basis sets were used.

4.4 Discussion

In this paper the two main focuses have been the shifting of the vibrational modes of pyridine due to the borane group in borane pyridine and the shifting of the vibrational modes of pyridine due to hydrogen bonding in water, and the characterization of the B-N bond in borane pyridine. As shown in figure 4.1.2 the first principle modes of pyridine

were measured experimentally at 991 and 1030 cm^{-1}, and the final mode was measured at 3057 cm^{-1}. The theoretical modes were scaled so the peaks in the theoretical calculations are usually only a few wavenumbers away from the experimental values. The experimental mode at 991 cm^{-1} corresponds to the theoretical mode at 978 cm^{-1} which is a difference of only 13 cm^{-1}, but the final experimental mode at 3057 cm^{-1} corresponds to a theoretical mode at 3074 cm^{-1} which is a difference of 17 cm^{-1}. Often in theoretical calculations plots are multiplied by a certain factor to create more accurate results when compared with experiment because theoretical calculations run on a harmonic oscillator model while real molecules exhibit anharmonic oscillations. The calculations with a B3LYP method seem to predict the first two modes at 991 and 1030 cm^{-1} more accurately and with greater intensity than the M06-2X calculations. The B3LYP calculations, shown in figure 4.1.8, did not predict the shape of the last mode as well as both calculations showed 2 or even 3 distinct peaks while the experimental mode only shows one peak. The M06-2X calculations, shown in figure 4.1.7, did a better job at predicting the shape of the mode, but were about the same distance away from the experimental peak as the B3LYP calculations. Overall the theoretical modes agree with the experimental modes better in shape with a M06-2X method, but most methods seem to be about the same distance away from the experimental modes.

When pyridine is interacting with a borane group, as in borane pyridine, it causes its modes to be shifted to higher energies. This is seen in figure 4.2.2 where the pyridine modes at 991 and 1030 cm^{-1} are shifted to 1023 and 1092 cm^{-1}. It is also seen in figure 4.2.3 where the final pyridine mode is shifted from 3057 cm^{-1} to 3088 cm^{-1}. This shifting to higher energies is often referred to as a “blue shift” so it would be fair to say that

pyridine's vibrational modes were blue shifted by the borane group in borane pyridine. Borane pyridine's modes were also higher in theoretical calculations than in experiment, and some correction factor could be used here as well. The B3LYP calculations, shown in figure 4.2.6, on borane pyridine also seemed to predict the first 2 modes better than the M06-2X calculations, shown in figure 4.2.7, as the M06-2X modes were very weak. However, The M06-2X/aug-cc-pVTZ calculation, shown in figure 4.2.9, almost exactly matched the shape of the experimental mode while the B3LYP calculations did not match as closely at all. As seen in pyridine the calculated modes were all about the same distance away from the experimental modes, except in the B-H stretching modes where the B3LYP calculations, shown in figure 4.2.10, are noticeably closer than the M06-2X modes in figure 4.2.11. The experimental B-H stretching modes were very wide and not very distinct so none of the calculations replicated the experimental mode exceptionally well.

In comparison to the shift by the borane group pyridine's modes were not shifted as much by its interaction with water, but the modes were still shifted in the same direction. The shifts, shown in figures 4.3.2 and 4.3.3, from pyridine to pyridine and water at a mole fraction of 0.3, which was the highest amount of water used, are small generally being below 10 cm^{-1}. After increasing the mole fraction by 0.1 from the initial mole fraction of 0.9 the shifting of modes did not show a large difference after a mol fraction of 0.5, so no samples were taken after χ=0.3. The shift of the first 2 modes is only from 991 and 1030 cm^{-1} to 1000 and 1033 cm^{-1}, which is a much smaller shift than the shifts in borane pyridine. The final and largest shift in pyridine and water, shown in figure 4.3.3, was from 3057 cm^{-1} to 3070 cm^{-1}, which is also a small shift. The theoretical pyridine and water calculation was most likely the most accurate calculation with respect to position after scaling. The

method and basis set used for this calculation was M06-2X/aug-cc-pVTZ as in a previous Hammer group paper it was said that this combination gives comparable results to the CCSD(T) method. The issue with this calculation is that it did not replicate the shape of any of the modes very well. For the first two pyridine modes the theoretical calculation, shown in figure 4.3.8, barely shows the first mode, and it may not show it at all since it is attached to the second mode. The calculation replicates the last mode better, but it still does not exactly agree with its shape. Finally, the experimental spectrum of pyridine and water (χ=0.5) shows a very long, broad peak at the end of the spectrum that can be seen best in figure 4.3.7. This peak is attributed to hydrogen bonding, and while the theoretical calculation does show this shift it does not replicate its shape very well. the theoretical peak is narrow while the experimental peak is very long with little distinction at lower mole fractions. This may be due to the fact that only one water molecule was used in the calculation.

The second main focus of this paper was the characterization of the B-N bond in borane pyridine. The M06-2X/aug-cc-pVTZ calculation agreed with the experimental data very well as the experimental B-N stretch occurs at 719 cm^{-1} and the theoretical B-N stretch occurs at 687 cm^{-1}. While this calculation agreed with the experimental data very well it also has very small peaks. This value is greater than some B-N stretches, like the one in the MIDA ester, in frequency while also being lower than other molecules, like ammonia borane. The B-N stretch in this molecule seems to be at a medium frequency in the range of B-N stretches since it's not too high or low.

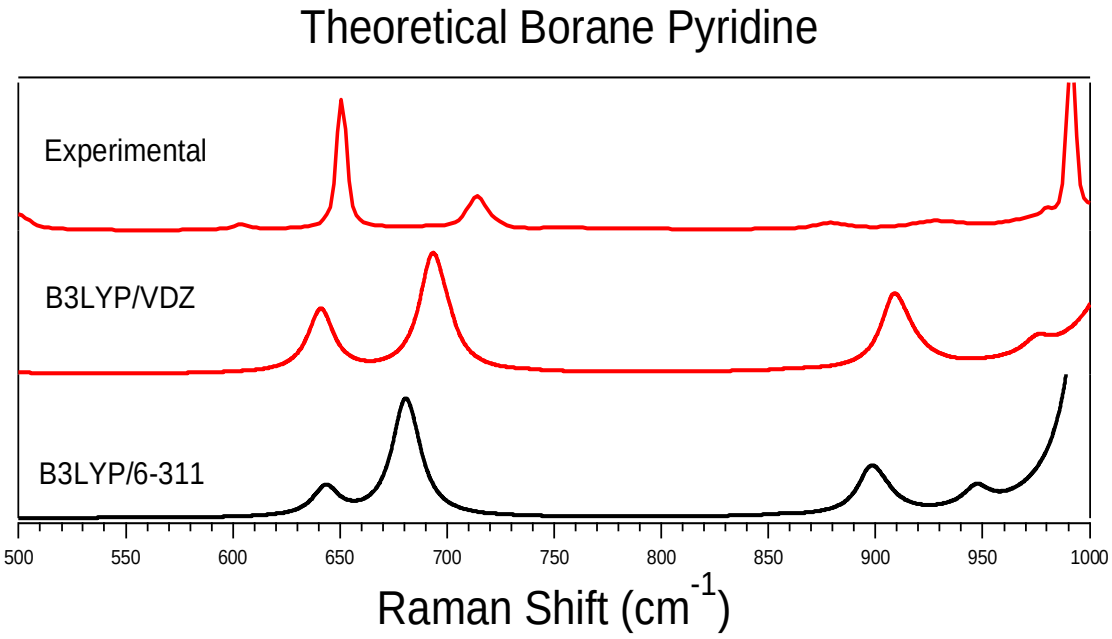

Figure 4.4.1- A figure showing the experimental and theoretical B-N stretch. The theoretical mode occurs at 704 cm^{-1} while the experimental shift occurs at 719 cm^{-1}.

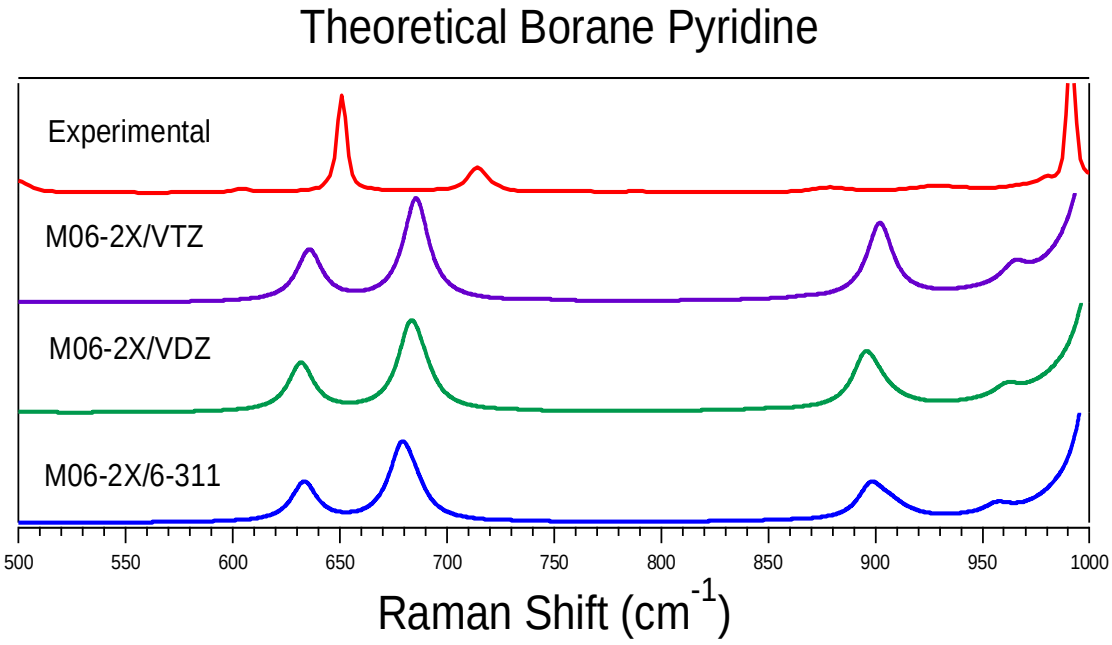

Figure 4.4.2- A figure showing the experimental and theoretical B-N stretch. The theoretical mode occurs at 687 cm^{-1} while the experimental shift occurs at 719 cm^{-1}.

4.5 Conclusions

Pyridine experiences shifts in its vibrational modes when interacting with a borane group as in borane pyridine, or when it interacts with water due to hydrogen bonding. The shifts experienced from borane pyridine are larger than the shifts experienced from water, most likely because the borane group interacts with pyridine through a covalent bond instead of just an intermolecular bond like hydrogen bonding. Both the addition of a borane group and hydrogen bonding blue shift the vibrational modes of pyridine, but the borane group blue shifts the modes significantly more. The B-N stretch in the borane pyridine molecule was characterized at 719 cm^{-1} experimentally, and theoretical calculations supports this claim as the M06-2X/aug-cc-pVTZ calculation found the B-N mode to be 687 cm^{-1}.

Chapter 5: References

(1) Tro, N. J. (2014). *Chemistry: A molecular approach*. Boston, Columbus: Perarson Education.

(2) Krishnan. (2007). POLAR AND NONPOLAR COMPOUNDS. Retrieved March 5, 2019, from http://users.stlcc.edu/gkrishnan/polar.html

(3) Winter, M. (n.d.). Boron: Electronegativity. Retrieved March 5, 2019, from https://www.webelements.com/boron/electronegativity.html

(4) Lindahl, P. A. (2012). Metal–metal bonds in biology. *Journal of Inorganic Biochemistry,106*(1), 172-178. doi:10.1016/j.jinorgbio.2011.08.012

(5) Reinemann, D. N., Wright, A. M., Wolfe, J. D., Tschumper, G. S., & Hammer, N. I. (2011). Vibrational Spectroscopy of N-Methyliminodiacetic Acid (MIDA)-Protected Boronate Ester: Examination of the B–N Dative Bond. *The Journal of Physical Chemistry A,115*(24), 6426-6431. doi:10.1021/jp112016j

(6) Wright, A., Hammer, N., Tschumper, G., 2012. Computational and Spectroscopic Studies of the Effects of Weak Intermolecular Interactions in Ammonia Borane.

(7) Clark, J. (2017, February 10). The Beer-Lambert Law. Retrieved March 7, 2019, from https://chem.libretexts.org/Bookshelves/Physical_and_Theoretical_Chemistry_Textbook_Maps/Supplemental_Modules_(Physical_and_Theoretical_Chemistry)/Spectroscopy/Electronic_Spectroscopy/Electronic_Spectroscopy_Basics/The_Beer-Lambert_Law

(8) The Electromagnetic Spectrum. (2016, May 22). Retrieved March 7, 2019, from https://www.miniphysics.com/electromagnetic-spectrum_25.html

(9) Al Shara, S. (2011, April). (PDF) Schrödinger cat states and single runs for the ... Retrieved March 3, 2019, from https://www.researchgate.net/publication/13376696_Schrodinger_cat_states_and_single_runs_for_the_damped_harmonic_oscillator

(10) LaVision. (n.d.). Retrieved March 07, 2019, from https://www.lavision.de/en/techniques/mie-rayleigh-raman/

(11) Kim, Y., Jeong, S., Jun, B., et al. (2017). Endoscopic imaging using surface-enhanced Raman scattering. *European Journal of Nanomedicine*, 9(3-4), pp. 91-104. Retrieved 22 Mar. 2019, from doi:10.1515/ejnm-2017-0005

(12) Case Study: Vibrational Frequencies of Ethylene. (n.d.). Retrieved March 11, 2019, from http://shodor.org/succeed-1.0/compchem/labs/vibrations/

(13) Bakker, J. M., Aleese, L. M., Meijer, G., & Helden, G. V. (2003). Fingerprint IR Spectroscopy to Probe Amino Acid Conformations in the Gas Phase. *Physical Review Letters,91*(20). doi:10.1103/physrevlett.91.203003
(14) Rulli, C. (n.d.). The Raman Spectrophotometer. Retrieved March 11, 2019, from https://www.sas.upenn.edu/~crulli/TheRamanSpectrophotometer.html
(15) Ferraro, J. R., Nakamoto, K., & Brown, C. W. (2009). *Introductory Raman spectroscopy*. Amsterdam: Academic Press.
(16) Quantum Properties of Light. (n.d.). Retrieved March 25, 2019, from http://hyperphysics.phy-astr.gsu.edu/hbase/optmod/qualig.html
(17) *Parr, R. G.; Yang, W. (1989). Density-Functional Theory of Atoms and Molecules. New York: Oxford University Press. ISBN 978-0-19-504279-5.*
(18) McNamara, L. (2016, January 14). *Louis McNamara's answer to* What is B3LYP and Why is it the most popular functional in DFT? Retrieved from https://www.quora.com/What-is-B3LYP-and-why-is-it-the-most-popular-functional-in-DFT
(19) For m06-2x Taylor, DeCarlos E.; Ángyán, János G.; Galli, Giulia; Zhang, Cui; Gygi, Francois; Hirao, Kimihiko; Song, Jong Won; Rahul, Kar; Anatole von Lilienfeld, O. (2016-09-23). "Blind test of density-functional-based methods on intermolecular interaction energies". The Journal of Chemical Physics. 145
(20) Y. Zhao & D.G. Truhlar (2006). "The M06 suite of density functionals for main group thermochemistry, thermochemical kinetics, noncovalent interactions, excited states, and transition elements: Two new functionals and systematic testing of four M06-class functionals and 12 other functionals". *Theor Chem Acc*. **120** (1–3): 215–241
(21) Engel, T., Reid, P., & Hehre, W. (2013). *Physical chemistry*. Boston: Pearson.
(22) Williams, A. (2017). *Spectroscopic and Computational Studies of the Hydrogen Bonding Interactions of Hydroxyethyl Ethers*(Unpublished master's thesis). The University of Mississippi.
(23) Weber, M. J. (1999). *Handbook of laser wavelengths*. Boca Ratón, FL: CRC Press.